Univerzita Karlova v Praze
Přírodovědecká fakulta
Ústav petrologie a strukturní geologie

Volcanic-hosted massive sulfide deposits: structure, origin and examples from the Iberian Pyrite Belt

Sulfidová ložiska vázána na vulkanity: struktura, vznik a příklady z iberského pyritového pásu

Bakalářská práce

Ondřej Krátký

Vedoucí práce: **doc. David Dolejš, Ph.D.**

Praha 2015

Prohlašuji, že jsem tuto bakalářskou práci vypracoval samostatně a výhradně s použitím citovaných pramenů, literatury a dalších odborných zdrojů. Tato práce ani její podstatná část nebyla předložena k získání jiného nebo stejného akademického titulu.

V Praze, 21. 8. 2015,

Ondřej Krátký

English abstract

The volcanic-hosted massive sulfide deposits (VHMS) represent one of the key deposit types in the modern world. Due to their polymetallic composition (Zn, Pb, Cu, Ag, Au and Sn in some cases) they are important source of the base metals as well as the precious metals. They have been forming through the Earth's history and are actively forming even now on a modern sea-floor through emanations of hot metal-bearing fluids. Extensive study of the volcanic-hosted massive sulfide deposit began in 1960s after discovery of active seafloor vents on the bottom of the Red Sea (e.g. Miller et al., 1966) in form of black smokers. They represent channels and are results of emanation of the hydrothermal fluids into the water column and actual evidence of the hydrothermal processes. Hydrothermal fluids were enriched in various elements, including base and precious metals. Certain elements (specifically metals) were leached from the host rock (volcanic and sedimentary) by the percolating seawater. This seawater was heated and modified into hydrothermal fluid by a heat from a magmatic intrusion, which represents the driving force of the whole hydrothermal system. This intrusion can be of variable composition – from basic to felsic. Sometimes fluids that are produced by this intrusion are also enriched in metals and produce a metal enrichment in the hydrothermal system. But this phoneme is rare and documented only from a few deposits (Kid Creek, Neves-Corvo). Active hydrothermal activity leads to precipitation of sulfide minerals and creation of a massive sulfide body. Precipitation can occur directly in the seafloor or bellow in the unconsolidated sediments (resulted from a mechanical collapse of the black smoker). Favorable environments for creation such accumulations are depressions on the seafloor – rifts, grabens or calderas. Massive sulfides can there be easily covered with sediments and thus preserved in the geological record. Hydrothermal fluids not only produce mineralization, which is spatially limited, but also large alteration zones. They are divided into *(i)* regional and *(ii)* local alteration zones directly linked to the mineralization processes. The stockwork zone is situated in the center of the local alteration zone (pipe-like alteration zonation). It represent the feeder zone for the whole VHMS system.

The Iberian Pyrite Belt is located on the Iberian Peninsula both in the Spain and Portugal. Its total tonnage and density of massive sulfide accumulations is extraordinary and unique compared to the other districts around the world. Two world-class massive sulfide deposits, the Aljustrel and the Neves-Corvo from the Iberian Pyrite Belt were studied in this thesis and both show many similarities. They are hosted by the volcano-sedimentary sequence and its felsic

units and both were formed before approximately 350Ma. They are interpreted to be result of a long-lived hydrothermal system with particularly efficient deposition mechanisms. Source of the metals for the whole belt was the Phyllite-Quartzite group and its unknown basement. But at the Neves-Corvo deposit there is a strong evidence for the magmatic fluid contribution into the system. This produced the bornite zone and cassiterite ores. But this phenomena (at the Iberian Pyrite Belt) is present only at the Neves-Corvo deposit.

České shrnutí

Vulkanosedimentární masivně sulfidická ložiska představují jeden z klíčových ložiskových typů v dnešním světě. Vzhledem k jejich polymetalickému složení (Zn, Pb, Cu, Ag, Au a Sn v některých případech) jsou důležitým zdrojem základních i cenných kovů. Tato ložiska vznikala napříč historií Země a vznikají i dnes v moderních oceánech díky emanacím hydrotermálních roztoků bohatých na kovy. Rozsáhlý výzkum vulkanosedimentárních masivních sulfidických ložisek začal šedesátých letech 20. století po objevení aktivního hydrotermálního sytému na dně Rudého moře (Miller et al., 1966) v podobě takzvaných černých kuřáků. Ty představují přívodní dráhu a vlastní výsledek emanací hydrotermálních roztoků do volného moře a jsou tudíž hmatatelným důkazem této aktivity. Hydrotermální roztoky jsou obohacené různými prvky, nevyjímaje základní a vzácné kovy. Převážně metalické prvky byly získány (loužením) z okolních hornin (jak vulkanických, tak sedimentárních) díky perkolující mořské vodě. Tato mořská voda byla důsledkem zahřívání modifikována v hydrotermální roztok. Teplo nutné k tomuto procesu pochází magmatické intruze, která představuje hlavní „motor" celého hydrotermálního systému. Tato intruze může být variabilního složení – od bazické po kyselou. V některých případech hydrotermální roztoky vyprodukované přímo magmatickou intruzí, které jsou také obohaceny kovy, způsobí navýšení obsahu kovů v celém hydrotermálním systému. Tento fenomén je však vzácný a byl zdokumentován pouze na několika ložiscích (Kid Creek, Neves-Corvo). Aktivní hydrotermální aktivita vede ke srážení sulfidických minerálů a jejich ukládání, což vede k vytvoření masivně-sulfidického tělesa. Tato tvorba a akumulace sulfidů může probíhat přímo na mořském dně, či v nezpevněných sedimentech (mnohdy následek kolapsu černého kuřáku). Příhodné geologické prostředí pro akumulaci sulfidických minerálů jsou deprese na mořském dně – riftové a grabenové systémy či kaldery. Masivní sulfidy uložené v těchto depresích mohou po sedimentaci být lehce překryty klastickým materiálem a tím pádem lépe zachovány v geologickém záznamu. Prostorově omezená depozice sulfidických minerálů není jediný výsledek činnosti hydrotermálních roztoků. Dalším, a neméně důležitým, je vytvoření rozsáhlých alteračních zón, které mohou být *(i)* regionální a *(ii)* lokální - přímo spojené s mineralizačními procesy. Uprostřed lokální alterační zóny je lokalizován žilník, který představuje přívodní kanál pro hydrotermální roztoky.

Iberský pyritový pás je situován na Iberském poloostrově jak ve Španělsku, tak v Portugalsku. Celkový objem rudy a hustota ložisek z něj činí výjimečnou oblast v porovnání s jinými rudními revíry. Dvě světově významná ložiska – Aljustrel a Neves_Corvo nacházející se v Iberském pyritovém pásu, byla v této práci studována a obě vykazují mnoho podobností. Obě jsou situována ve vulkano-sedimentární sekvenci, konkrétně jsou vázána na její kyselé členy a obě se zformovaly přibližně před 350Ma. Jsou interpretovány jako výsledek dlouhotrvajícího a efektivního (co se tvorby a depozice sulfidových minerálů týče) hydrotermálního systému. Jako zdroj kovů byla pomocí izotopových studií určena podložní fylito-kvarcitová jednotka a její neznámé podloží. Avšak, na ložisku Neves-Corvo existují přímé důkazy, že jako zdroj kovů posloužily i magmatické hydrotermální roztoky, které byly derivovány z podložní neznámé magmatické intruze. Ty daly vznik bornitové zóně a kasiteritovým rudám. Toto je však v celém regionu dokumentováno jenom na ložisku Neves-Corvo.

Table of Contents

1. Introduction

1.1. Volcanic-hosted massive sulfide deposits

Volcanic-hosted massive sulfide mineralization styles, also known as VHMS (volcanic-hosted massive sulfide) or VMS (volcanogenic massive sulfide) deposits, are thoroughly studied ore deposit type due to their economic importance and general geological interest. This name distinction is often referring to the host-rock description and mechanism of formation, respectively. By definition, these are strata-bound accumulations of sulfide minerals that precipitated at or near the seafloor and in spatial, temporal and genetic association with contemporaneous volcanic activity (Franklin et al., 1981; Herzig and Hannington, 1995; Barrie and Hannington, 1999; Large et al., 2001). They form through the focused discharge of hot, metal-rich hydrothermal fluids emanating from the seafloor. Thus, the VHMS deposits are classified in the general class with heading of “exhalative” deposits, which also includes sedimentary exhalative (SEDEX) and sedimentary nickel deposits (Eckstrand et al., 1995). But in some cases, massive sulfide accumulations don’t form on the ocean-floor directly, but develop as a shallow sub-seafloor replacement. This occurs when hydrothermal fluids infill primary pore space in either extrusive, autoclastic, volcanoclastic, or epiclastic succession bellow an impermeable cap (Galley et al., 2007). They have been forming throughout the Earth’s history (documented from 3.4 Ga) and are actively forming in modern seas (Herzig and Hannington, 1995).

They are one of the major economic sources of Zn, Cu, Pb, Ag, and Au, and a significant source for Co, Sn, Se, Mn, Cd, In, Bi, Te, Ga, and Ge (Galley et al. 2007*)*. Some of the deposits are exploited for pyrite only and to produce sulfuric acid (Ridley 2013, pg. 183). The sulfide minerals typically occur in lenses (>60% sulfides) enclosed in a host rock, which can be either volcanic or sedimentary and or in veins forming the stockwork zone in the footwall strata. Many of the VHMS deposits contain two major structural components: tabular to mound-shape body, which primarily consists of massive sulfide (>40%), quartz and phyllosilicates, iron oxide minerals and altered silicate wall rock (Fig. 1.1). These strata-bound bodies are typically underlain by discordant to semi-concordant stockwork veins and disseminated sulfide mineralization (Galley et al., 2007). The stockwork system is enveloped by alteration halos, which are one of the exploration vectors for the VHMS deposits.

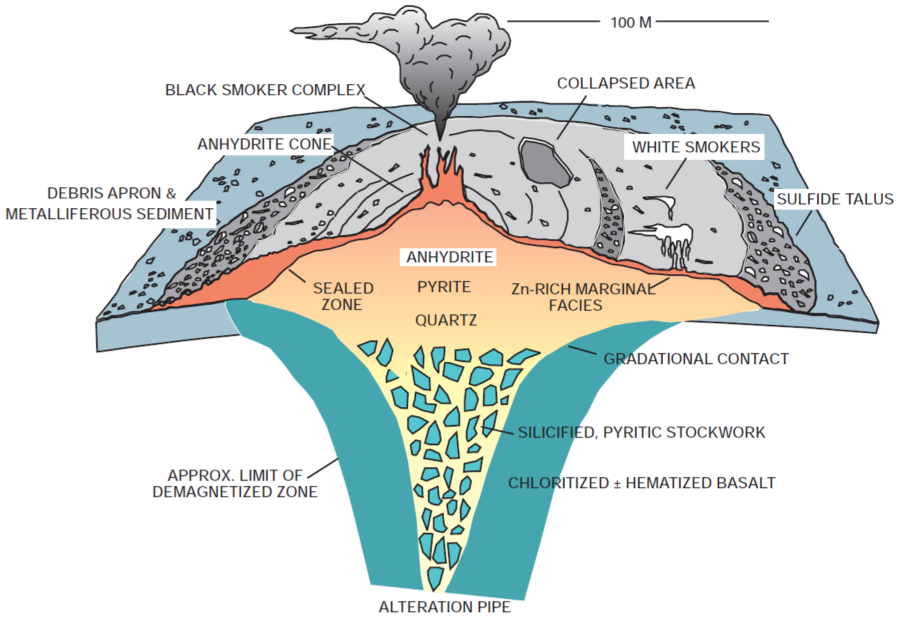

Figure 1.1. Schematic cross-section of the modern sulfide deposit from the Mid-Atlantic Ridge with concordant semi-massive to massive sulfide lens underlain by a discordant stockwork vein system which is associated with "pipe" type alteration halo (Hannington et al., 1998; Galley et al., 2007).

The VHMS deposits are classified by various criteria: (i) base-metal content, (ii) gold content, or (iii) host-rock lithology. The most common classification based on the base-metal content was proposed by Franklin et al. (1981) and later modified, for example, the Zn-Pb-Cu group was added by Large (1992), for better representation of the VHMS deposits of Australia.

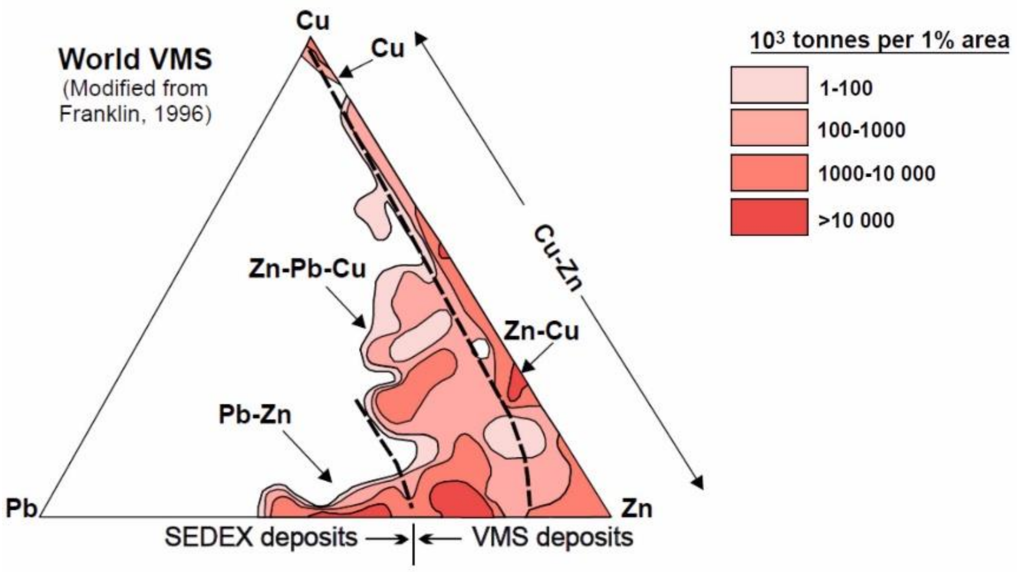

Figure 1.2. Base metal classification scheme of worldwide VHMS deposits as defined by Franklin et al. (1981) and modified by Large (1992) to include the Zn-Pb-Cu class (Galley et al., 2007).

Volcanic hosted massive sulfide deposits are divided into Cu-Zn, Zn-Cu and Zn-Pb-Cu groups based on their bulk base-metal ratios (Fig. 1.2). Large divided VHMS deposits generally into categories based on their size: giant (>100 Mt), very large (50-100 Mt) and large (25-50 Mt) respectively (Galley et al., 2007). Nevertheless tonnage of an average VHMS deposit is 1-3 Mt (Fig. 1.3) (e.g. Ohmoto, 1996).

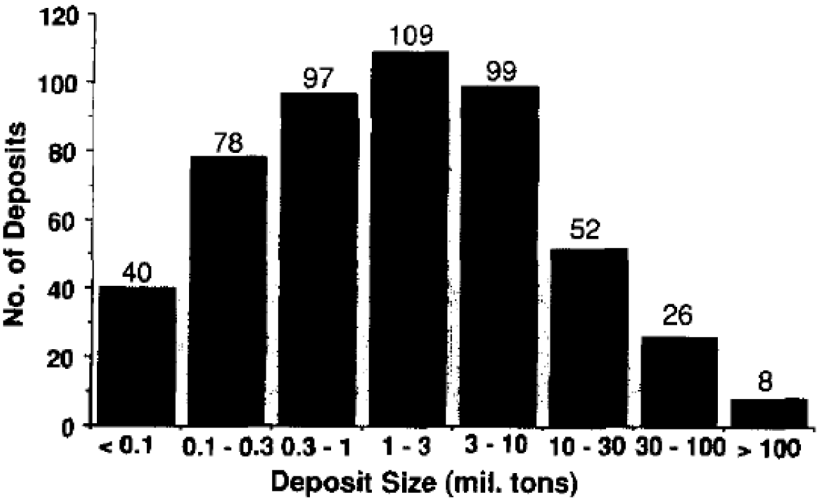

Figure 1.3. Tonnage distribution of 509 VHMS deposits worldvide (Ohmoto, 1996).

Most widely accepted classification was primary proposed by Barrie and Hannington (1999) and expanded by Franklin et al. (2005). Deposits are divided on a basis of the litostratigraphic composition into five types:

- Mafic: this deposit type is predominantly mafic (>75%) and contains no or very absent (<1%) felsic rocks with minor siliciclastic or ultramafic (<10%) rocks. It includes ophiolite settings almost exclusively in Phanerozoic rocks. On average they are Cu-rich and Pb-poor in comparism to other types. Deposits of the Newfoundland Apalachinas, Cyprus, Oman are included in this group.
- Bimodal-mafic: this deposit type is defined as having >50% of mafic and >3% of felsic rocks. Siliciclastic rocks are subordinate. Host-rock composition reflects mostly primitive volcanic arc or rifted primitive volcanic arc settings. This type includes Noranda district, Quebec (Gibson and Watkinson, 1990) and Flin Flon deposit (Syme and Bailes, 1993). It is the most comon VHMS type.
- Mafic-siliciclastic: this type of deposit has subequal proportions of mafic volcanic or intrusive rocks and turbiditc siliciclastic rocks. Felsic volcanic rocks are minor or

absent. They may contain significant proportion of carbonate. Type examples are the Besshi deposit of Japan and the Windy Craggy deposit of British Columbia, Canada.

- Bimodal-felsic: this deposit type has >50% felsic rocks and <15% silicislastic rocks. Mafic rocks are subordinate. They are found in mature volcanic arcs or rifted arc settings. Typical examples are the Hokuroku district, Japan (Ohnoto and Skinner, 1983) and the Rosbery deposir, Tasmania (Green et al., 1981). On average, they contain the most Zn and Ag of all five deposit types.
- Bimodal-siliciclastic: this deposit type has (aproximately) equal proportion of volcanic (more felsic than mafic) and siliciclastic rocks. Iberian Pyrite Belt of Portugal and Spain and the Bathurst camp, Canada are typical examples. They represent the greatest tonnage and the largest average deposit size. They have the lowest Cu and highest Pb content.

Geographical distribution of VHMS deposits is variable, partly due to their incorporation in the tectonostratigraphic record (commencing at 3.4 Ga in the Pilbara Block, Australia) to actively forming precipitates on the modern oceanic crust. These deposits are found on all continents, except Antarctica, although the Zn-Pb-Cu deposits are forming in the Bransfield Strait adjacent to the Antarctic Peninsula (Fig. 1.4) (Petersen et al., 2004). The over 800 VMS deposits worldwide range in size from 200 000 tons of ore to supergiant deposits containing more than 150 million tons (Franklin et al., 2005). The largest deposit is Rio Tinto in the Spanish part of the Iberian Pyrite Belt with more than 1.575 Bt of ore.

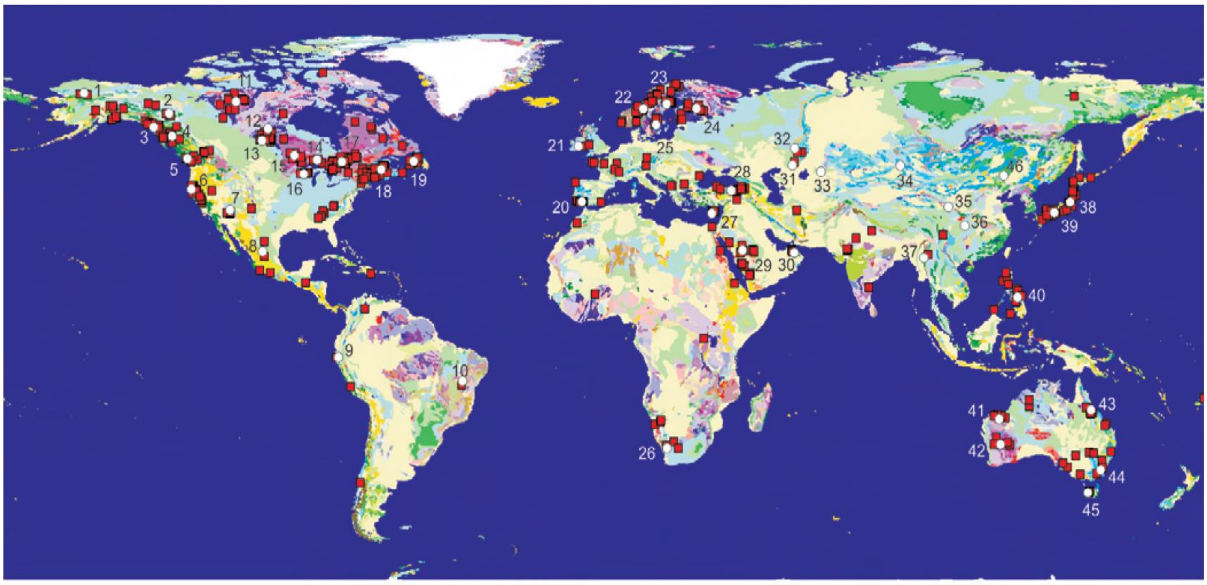

Figure 1.4. Geographical distribution of ancient VHMS deposits. Data about tonnage are in Table 1.1 (Sinclair et al., 1999; Franklin et al., 2005).

Table 1.1. Tonnage of the main VHMS deposits/districts in the world (Sinclair et al., 1999; Franklin et al., 2005)

No.*	Deposit/District, Country	Tonnage (Mt)	No.*	Deposit/District, Country	Tonnage (Mt)
1	Brooks Range, Alaska	35	23	Skellefte, Sweden	70
2	Finlayson Lake, Qukon	20	24	Outokumpu-Pyhasalmi, Finland	90
3	Windy Craggy, BC & Green´s Creek, Alaska	300	25	Bergslage-Orijarvi, Sweden & Finland	110
4	Northern Cordillera, British Columbia	100	26	Preiska, South Africa	45
5	Myra Falls, British Columbia	35	27	Troodos, Cyprus	35
6	Shasta, California	35	28	Black Sea, Turkey	200
7	Jerome, Arizona	40	29	Saudi Arabia	70
8	Central Mexico	120	30	Semail, Oman	30
9	Tambo Grande, Peru	200	31	Southern Urals, Russia / Kazahstan	400
10	Amazonian craton, Brazil	35	32	Central Urals, Russia	100
11	Slave Province, Northern Territories, Nunavut	30	33	Rudny Altai, Kazahkstan / Russia	400
12	Ruttan, Manitoba	85	34	Altai Shan, Mongolia	40
13	Flin Flon-Snow Lake, Manitoba	150	35	North Qilian, China	100
14	Geco, Manitouwadge, Ontario	60	36	Sanjiang, China	50
15	Sturgeon Lake, Ontario	35	37	Bawdwin-Laochang, Burma	40
16	Ladysmith-Rhinelander, Wisconsin/Michigan	80	38	Hokuroku, Japan	80
17	Abitibi, Ontario-Quebec	600	39	Besshi, Japan	230
18	Bathurst, New Brunswick	495	40	Phillipines arc	65
19	Dunnage Zone, Newfoundland	75	41-42	Pilbara, Yilgarn Western Australia	75
20	Iberian Pyrite Belt, Spain & Porutgal	1575	43	Central Quensland, Australia	80
21	Avoca, Ireland	37	44	Lachlan Fold Belt, Australia	100
22	Trondhjeim, Norway	100	45	Mt. Read, Tasmania	200
			46	Sino-Korean Platform	40

*numbers refer to Figure 1.4., tonnage is approximate

1.2. Structure and content of the thesis

In this thesis I have focused on the description of the main factors, which lead to creation of the massive sulfide deposit and comparison of the two deposits located in the Iberian Pyrite Belt – the Aljustrel deposit and the Neves-Corvo deposit. Each deposit and each mining district is unique and still they all have something in common. I was trying to identify and describe these similarities (environment of formation, source of fluids, alteration zoning) and things in which they differ (mineralogical composition, extent of the alteration zone). By comparing these two deposits and the whole Iberian Pyrite Belt with rest of the world, I was able to trace these features and also better understand the main driving forces, which can lead to formation of a economic massive sulfide accumulation.

This thesis is mainly a recherché work with minor original data - microprobe analysis of chlorite and sericite samples from the Aljustrel deposit. This work consists of three main parts; first is focused on a description of the main features that have all VHMS deposits in common – typical tectonic environments of formation, types of the host-rocks, alteration styles, geochemistry and mineralogical composition. By studying this features over more than a century, we have now generally good idea how this deposits were forming, what were the main driving forces and parameters that were affecting each deposits during its formation. Studying deposits *in situ* and later discovery of active forming accumulations on a modern sea-floor are the main sources of data. Second part is then dedicated to the Iberian Pyrite and to two deposits situated at Portugal side – the Aljustrel deposit and the Neves-Corvo deposit. Finally the third part, the Interpretation and Discussion, is then focused on the comparison of both studied deposits. Their main analogs and differences, as well as on the comparison of the Iberian Pyrite Belt with the rest of the world

I had the opportunity to study these issues thanks to the Erasmus program at the Universidade de Lisboa in Portugal, one of the centers for the research of the Iberian Pyrite Belt.

2. Geological setting and alteration styles

2.1. Setting of volcanic-hosted sulfide deposits

Geological settings of the VHMS deposits are rather variable but always associated with submarine volcanic activity (Ridley 2013, pg. 189-190):

- Ophiolites – fragments of oceanic crust underlid by ultramafic upper mantle. In sequences of pillow basalts or at basalt-sediment occurs for instance Cyprus deposit (Constantinou and Govett, 1978; Adamides, 2010). This is also known as the Cyprus type of deposit.
- Greenstone belts of Archean and Early Proterozoic age, which include a wide range of deformed and metamorphosed rocks mafic and felsic igneous rocks. Examples are Kidd Creek, Ontario, Canada (Hannington and Barrie, 1999), Crandon, Wisconsin, USA (DeMatties, 1994), and Panorama, Western Australia (Vearncombe et al., 1995).
- Mafic to felsic submarine sequences interbedded with turbidites and shales – these successions occur in deformed terrains where they form belts. Many of these volcanic belts formed during convergent-margin tectonics. This setting include submarine volcanic arcs – Kuroko district, Japan (Sato, 1977) and back-arc basins.
- Marine sedimentary successions, composed of turbidites and black shales with intercalated volcanic rocks. Deposits of this type are the Iberian pyrite belt, Spain and Portugal (Tornos, 2006), and Rammelsberg, Germany (Large and Walcher, 1999).

All VHMS deposits are associated with locally extensional stress regime accompanied by normal faulting. It includes rifting and arc environments – continental and nascent arc, rifted arc and back-arc settings (Franklin et al., 1998; Allen et al., 2002). It corresponds to sea-floor and simultaneous magmatic and volcanic activity (Fig. 2.1). Deposits from the arc settings, however, dominate in the geological record due to more favorable conditions for their preservation.

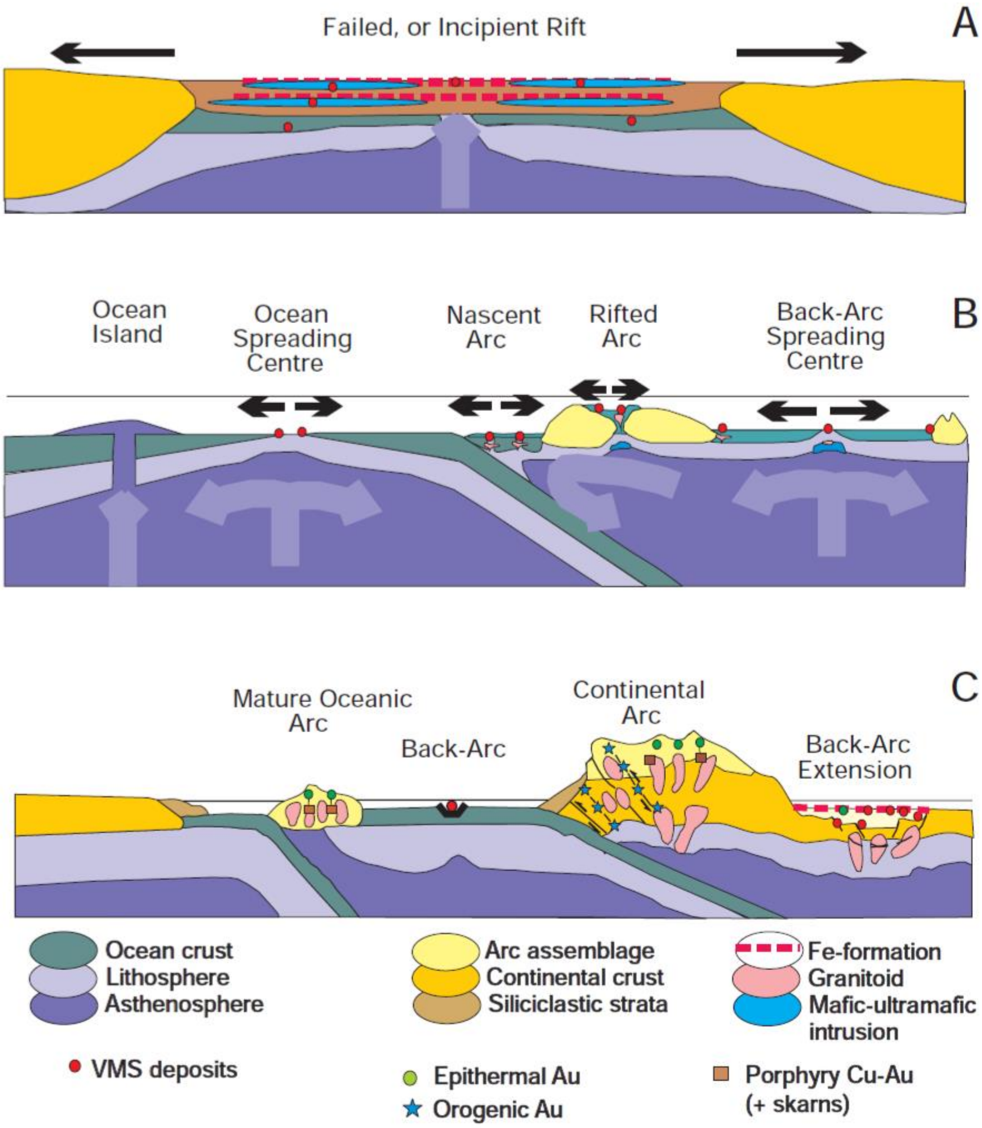

Figure 2.1. Principal tectonic environments of formation of the VHMS deposits in the Earth´s history: **A** – Early oceanic crust was dominated by rift environments in primitive basalts and/or komatiites. Basins were formed by incipient rifts and filled with siliciclastic material and associated Fe-formations; **B** – Oceanic spreading centers developed and they resulted in formation of oceanic basins. In these environments, VHMS deposit dominated by mafic rocks were formed. The development of subduction zones resulted in oceanic arc formation. These extensional domains are associated with bimodal mafic, bimodal felsic, and mafic-dominated VHMS deposits; **C** – mature arc and ocean-continent subduction zones resulted in arc assemblages that most of the felsic-dominated and bimodal siliciclastic deposits. Black arrows represent direction of extension and pale arrows represent direction of the mantle movement (Groves et al., 1998; Galley et al., 2007).

The dominant geological structures of the VHMS deposits are grabens, half-grabens and pull-apart basins and/or symmetrical or asymmetrical calderas. In the following text, I will use the calderas as the principal environment where economic accumulation of minerals occurs. Caldera collapse due to magma release leads to the formation of circular or elongate morphological depression bound by faults (Fig. 2.2). In extensional and transtensional settings, the main caldera faults may not be circular, but instead form a series of interconnected linear or arcuate structures (Kennedy, 2000). These faults and their intersection represent channels for influx of the sea-water into the system and its return as an ore-bearing fluid.

Originated subsidence is filled with pyroclastic material and marine sediments, which creates horizon permeable enough for migration of hydrothermal fluids toward the surface. These fluids are mobilized by heat from magmatic intrusion. Such deposition is observed at Myojin Knoll caldera, Japan, where a large VHMS deposit is actively growing above the main caldera fault (Fiske et. al., 2001).

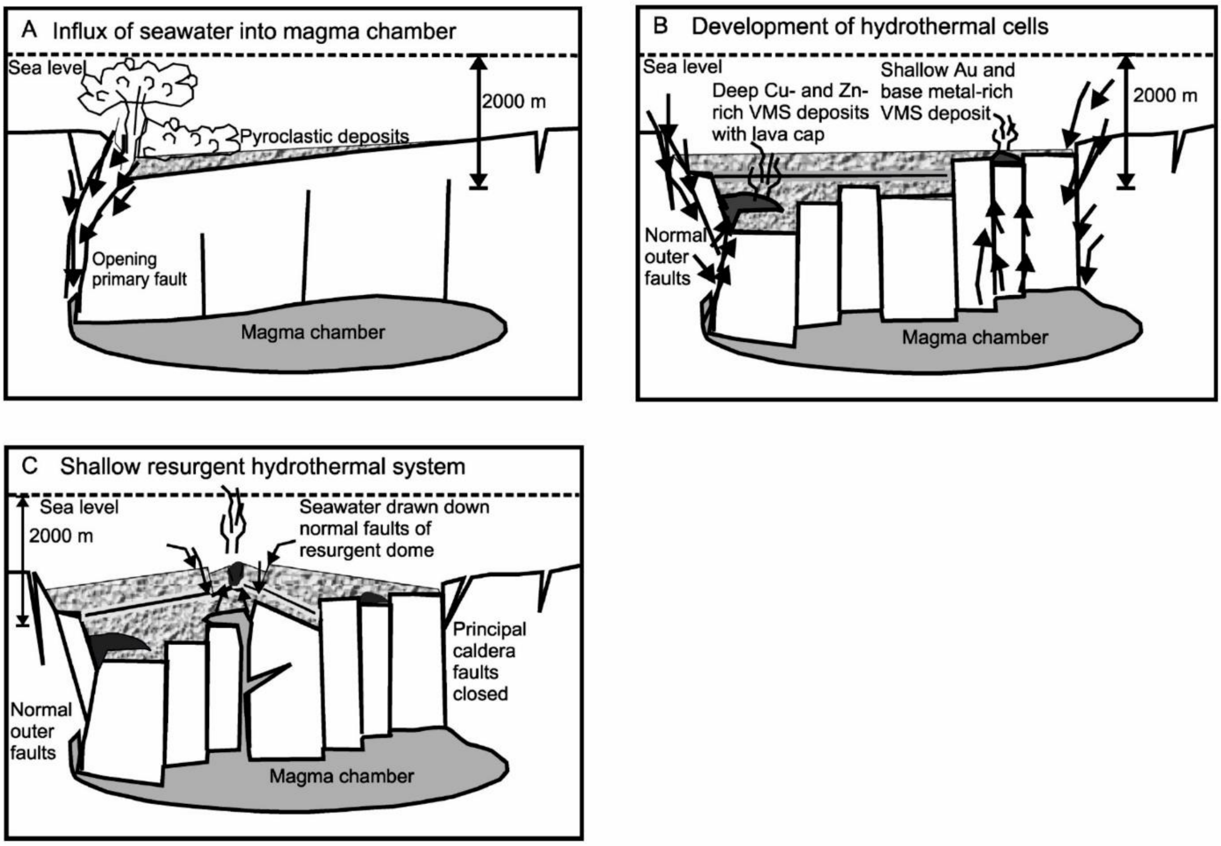

Figure 2.2. Conceptual view in space and time of caldera-related submarine magmatic-hydrothermal system (Stix et al., 2003).

Asymmetrical profile of these structures enables accumulation of sulfide minerals and their preservation in geological record. Due to steep slopes of these depressed environments, massive sulfide bodies can be covered with marine sediments (turbiditic flows) and pyroclastic from volcanic activity quickly. This “cover” protects nascent body from erosion and dispersion into the ocean mass. Subsequent re-deposition from oceanic crust onto continental and connected metamorphic activity leads to reprocessing of whole geological sequence. This disables closer identification of the formation environment of VHMS. Though, in geological record do exist deposits, where the evidence of caldera environment is clear: giant Archean Horne deposit (Gibson and Kerr, 1993; Kerr and Gibson, 1993), Hunter Mine caldera, Quebec (Mueller and Mortense, 2002). This criteria may be also used for Selbaie, Suturgeon Lake and Bergslagen deposit (Franklin et al., 1981). In these structures, we can find wide spectrum of ore deposits aside from the VHMS, for example porphyry Cu, epithermal veins, and polymetalic veins.

2.2. Shape, size and mineralogy of the VHMS deposits

The shape, size and mineralogical composition of the VHMS deposits is controlled by several main factors (Ohmoto, 1996):

- Chemical and physical characteristics of the seawater (later modified into ore-bearing fluid)
- Physical characteristics and a stage of development of the fault system. This structural inhomogeneity serves as a plumbing system for influx and distribution of hydrothermal fluids.
- Geothermal gradient in the host rocks and duration of the hydrothermal event, which is proportional to the size, magnitude and depth of the magmatic intrusion. The depth of emplacement varies from 2 to 4 km under the oceanic floor;
- Tectonic setting and topography of the submarine environment (caldera, pull-apart basin).

In the area of VHMS district, there is always more than one massive sulfide body. For example, massive caldera with more than one fault intersections or elongated magmatic center in rift environments, which leads to creation of several bodies There are several mathematical models which allowing us to calculate possibility and location of other massive sulfide body in the VHMS district (e.g. Mosier et al., 2007).

Accumulations of the massive sulfides are always inhomogeneous, mineralogical composition and distribution of minerals varies within the body. All VHMS deposits consist of two main units (Fig. 2.3): (*i*) stratiform or stratabound mound-shaped body, consisting of approximately ~50 % sulfides, and (*ii*) underlying stockwork system (or stringer zone), where the sulfide minerals are present in veins or disseminated in the host rock. The stringer zones mark the channels of hydrothermal fluid ascent (Roscoe, 1965; Williams et al., 1975), whereas the anastomosing veins are a result of a hydraulic fracturing of the host-rock.

The mound-shape body is a result of the accumulation of the sulfide minerals on the sea-floor or in unconsolidated sediments. Some accumulations but did not originate from sedimentation of sulfide minerals. They origin as a result of circulation of hydrothermal fluids in poruses of an unconsolidated sediments (volcanoclastic or siliciclastic) under the impermeable cap, which represents a boundary for the fluid circulation and surrounding environment. This process led to creation for example Horne No. 5 lens (Kerr and Gibson, 1993) or Kidd Creek (Hannington et al., 1999) deposits. Bodies of massive sulfides diverse in both shape and size – lenticular or podiform bodies, which are characterized by bands of minerals from centimeters to decimeters size and variable major sulfidic mineral. The stockwork system, which is underlying the massive sulfide body, is situated in the center of the hydrothermal alteration zone. Vertical range of this zone can be up to hundreds of meters, but mostly is twice the size of massive sulfide body.

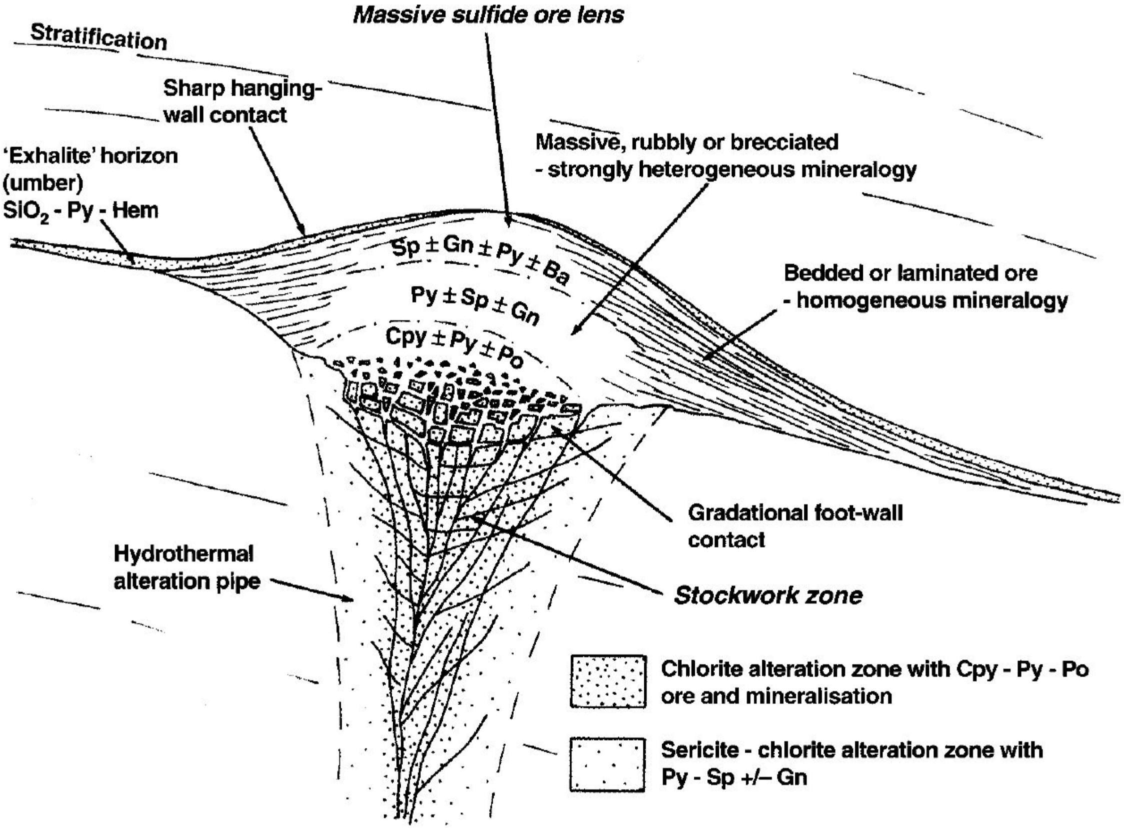

Figure 2.3. Idealized cross-section threw a massive sulfide lens. From Ridley (2013)

Metals come (mainly) from surrounding volcanic rocks, dissolved by the convection of the hydrothermal fluids percolating through them. At some deposits (Neves-Corvo) there is a strong evidence for magmatic fluid contribution, but this phenomena is very rare.

Specific mineral assemblages are result of a specific host-rock (e.g. Barrie and Hannington, 1999). The Cyprus-type VHMS deposits are for example typified by a Cu + Zn metal association, which reflect their formation by leaching of predominantly mafic volcanic rocks, whereas the felsic or mixed volcanic rocks associated with Kuroko-type deposits have a Pb + Zn + Cu metal association (Robb, 2005).

Mineralogy of the VHMS deposits is not very complicated. Main gangue mineral is quartz. It is present disseminated through the massive sulfide body and present in masses in the stockwork zone as a result of intense silicification. Due to intense hydrothermal alteration and changes in mineralogy of the host-rock, sericite and chlorite are present as the main alteration mineral phases after quartz. They are followed by barite and sulfate minerals, which are mainly present in the upper parts of the body (Fig. 2.4). In some deposits talc and/or magnetite can be observed at the bottom of the massive sulfide lens. Pyrite (FeS_2) is the dominant sulfide mineral. The principal hosts of copper are chalcopyrite ($CuFeS_2$), cubanite ($CuFe_2S_3$), and tennantite ($(Cu,Fe)_{12}As_4S_{13}$). Other economic metals are hosted in sphalerite (ZnS) and galena (PbS) (Ridley 2013, pg. 193-194). In some deposits, gold may be present as minute disseminations in the ore body.

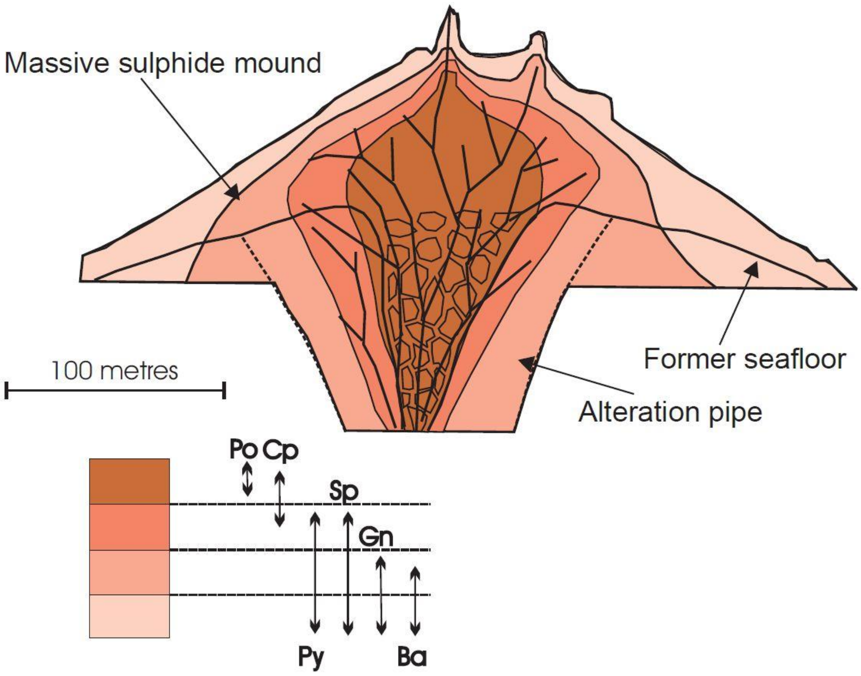

Figure 2.4. Commonly observed mineral zonation in VHMS bodies. Abbreviation: Ba-barite, Cp-chalcopyrite, Gn-galena, Po-pyrrhotite, Py-pyrite, Sp-sphalerite (Lydon, 1984).

2.3. Alteration styles and their spatial distribution

Hydrothermal alteration of a paleo-seafloor is a process which affects original volcanic rocks and produce changes in mineralogy, geochemistry and net volume (Barrett and MacLean, 1994). Zones affected by hydrothermal alteration connected with VHMS deposit include footwall alteration pipes, stratabound altered footwall zones and altered hanging wall zones (Gifkins et al., pg. 164). At significant number of deposits (approximately half of them) dominates pipe-like hydrothermal zone structure (Fig 2.5A). However at many districts pipes are less common and stratabound altered zone type dominates (Fig 2.5B). Hydrothermal alteration connected to the VHMS deposits is an epigenetic process. Horizontal extent of the alteration halo is from hundreds of meters to several kilometers away from the central stockwork zone.

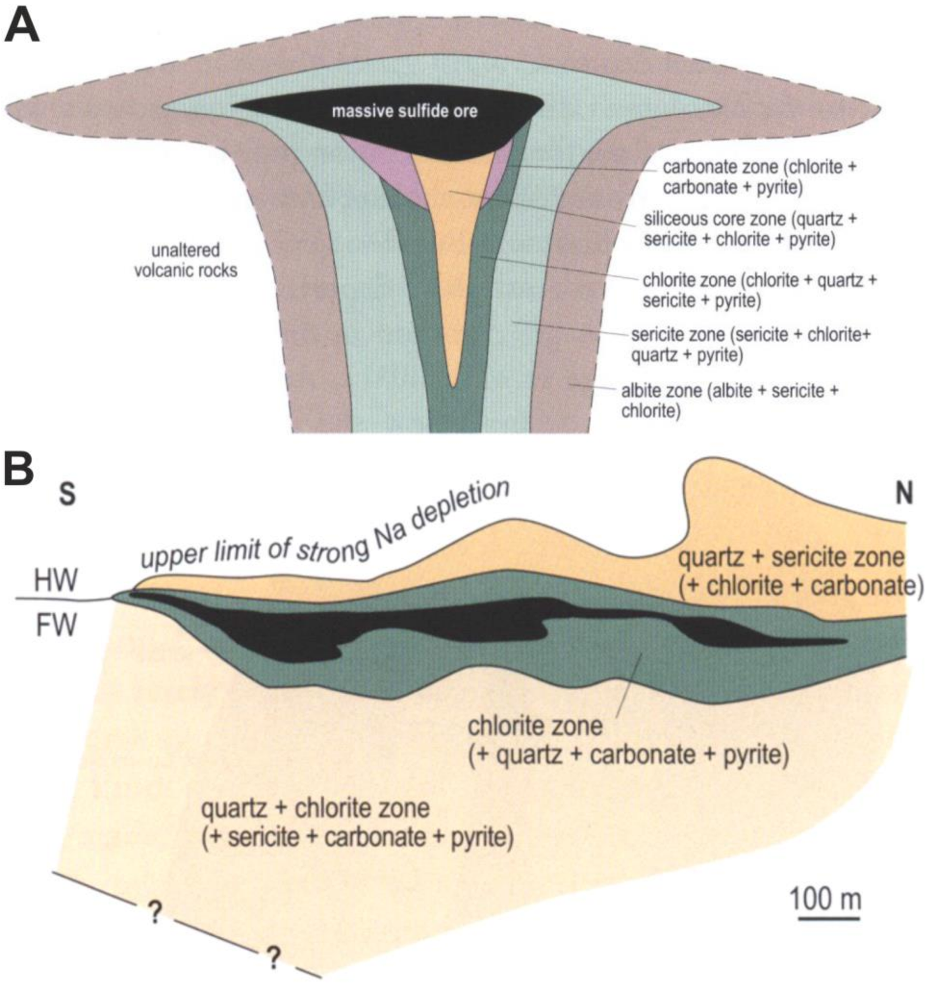

Figure 2.5. Different alteration zones of a VHMS systems; **A** represents idealized cross-section through a pipe-like alteration zones; **B** represents stratabound altered zones of the Scuddles deposit from Western Australia in a plan view. Abbreviations: HW=hanging wall and FW= foot wall (Gifkins et al., pg. 165 and 167)

I will use pipe-like footwall alteration zonation (Fig 2.5A) for the description of an alteration zoning, because it is much better understood and clear than the stratabound altered footwall zonation. Stratabound altered footwall zones have similar mineral assemblages to footwall alteration pipes, but the zones are distributed parallel to stratigraphy (Gifkins et al., pg. 167). Each alteration zone is dominated by different mineral. They include quartz, chlorite, sericite and albite (from the center outwards).

Siliceous core zone is situated in the center of the concentric alteration zone and represents the most intensively altered part. All primary textures of volcanic rocks have been destroyed. It consist mainly of quartz + pyrite + sericite ± chlorite assemblages (Gifkins et al., pg. 165). This zone is not present very often and was described only from a few deposits – Hellyer (Gemmel and Large, 1992), Brunswick No. 12 and other deposit from the Bathurst mining camp (Zhang et al., 2003).

Chlorite zone consists mainly from chlorite (>50% wt%) with subordinate quartz + pyrite + sericite ± carbonate (Gifkins et al., pg. 165). No volcanic or sedimentary textures are preserved due to intensive alteration processes. At some provinces this zone also hosts pyrite and chalcopyrite in vein-type mineralization (at the Iberian Pyrite Belt). Studies of chlorite composition indicate that inner chlorite zones are dominated by Mg-rich chlorite and Fe/Mg ratio increase from inner chlorite to more distal sericite zone (e.g. Riverin and Hodgson, 1980).

Sericite zone envelopes the inner chlorite (and siliceous if present) zone and is characterized by presence of sericite + chlorite + quartz + carbonate + pyrite assemblages (Gifkins et al., pg. 165). This zone is also intensively altered but with sparse relics of primary textures. At the outer margin of this zone it grades into least altered rocks. In many cases it is laterally extensive and merge with different alteration zones away from the central pipe.

Albite zone surrounds the sericite zone and consists of weakly altered rocks. Mineral assemblages include albite + chlorite ± sericite (Gifkins et al., pg. 165). It has been described only at several districts (Aljustrel - Iberian Pyrite Belt) and is important as one of the exploration vectors.

Alteration of hanging wall is in compare with the footwall alteration much less intense. Commonly observed mineral assemblages are sericite-rich. This zone occur mostly only several meters above the massive sulfide body.

3. Methodology

3.1. Microprobe analysis

Minerals were analyzed using in polished thin sections using the JXA-8200 (WD/ED combined microanalyser) microprobe from JEOL hosted at the Faculdade de Ciencias at the Universidade de Lisboa in Portugal.

3.2. Thin-sections observation and description

The minerals were studied in plane- and cross-polarized light and in reflected light for the opaque minerals. A camera attached to the microscope was used to take pictures of the minerals. The opaque minerals and mineral assemblages of each thin section were determined using the "Olympus BX60" optical microscope hosted at the Faculdade de Ciencias at the Universidade de Lisboa in Portugal. The opaque ore phases were analyzed in air, under reflected light with objectives of 5, 10 and 40x magnification.

Thin sections are selected in order to show several stages of mineralization process, specific ore types as well as the altered host rock. Thin sections from the Gavião ore body were prepared from one drill hole - SA 25. Thin sections from the Neves-Corvo were prepared from several drill holes and represent representative samples of majority of ore types and connected alteration styles.

4. Volcanic-hosted massive sulfide deposits of the Iberian Pyrite Belt

4.1. Geological setting

The Iberian Pyrite Belt is a world-class metallogenetic province situated at the SW of the Iberian Peninsula extending from Seville in Spain to the south of Lisbon in Portugal (Fig. 4.1). This province contains numerous Paleozoic volcanic-hosted massive sulfide deposits. Riotinto is the largest known massive sulfide deposit in the Iberian Pyrite Belt, and probably also in the world (Rona 1988). This highly productive VHMS belt contains more than 85 massive sulfide deposits with total mass exceeding 1600 Mt of massive ore (Leistel et al., 1998) to which more than 2000 Mt of low-grade stockwork mineralization should be added (García Palomero et al., 1993). The mineralization is distributed between eight supergiant and a significant number of other smaller deposits.

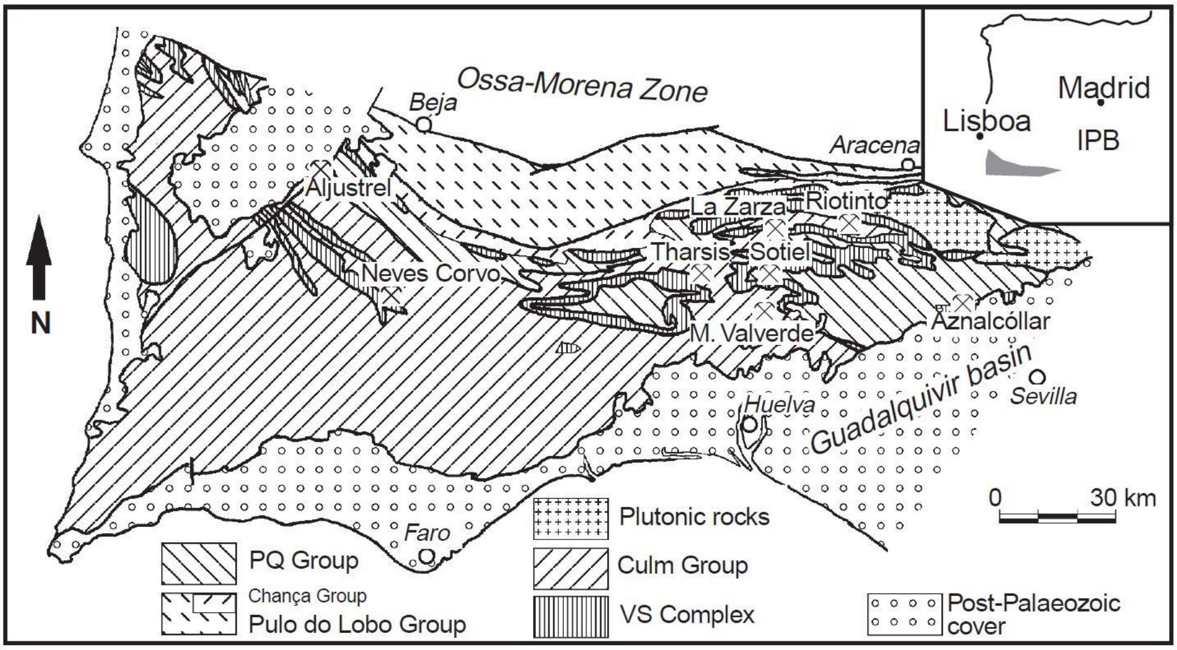

Fig. 4.1. Geological map of the Iberian Pyrite Belt (Carvalho et al., 1976).

Ore-forming events occurred during waning stage of felsic volcanism within a thin volcanic-sedimentary complex (VSC; 349.8 ± 0.9 to 356.2 ± 0.7 Ma; Barrie et al., 2002; Fig. 4.2). This VSC group (<600 m thick) consists of an altered felsic and mafic volcanic rocks within a mainly detritic sedimentary sequence of shales and volcano-derived sandstones (Sáez et al., 1999). VSC sequence is situated on the top of a thick sequence of shallow-platform siliciclastic sediments of the Phyllite-Quartzite group (>2000m thick) of the Upper Devonian age and older. This group is described as a monotonous sequence of shales and sandstones (Moreno and Sáez 1990). Both groups are then overlain by synorogenic flysch succession of the Baixo Alentejo Flysch Group (>1600 m thick) of the early to middle Carboniferous (Oliveira et al., 2006). The Culm Group represents an infill of turbidite sediments in a subsiding basin (Oliveira 1983) whose source areas would be both the Iberian Pyrite Belt and the eroding northerly units including the Ossa-Morena Zone of the Iberian Massif (Moreno, 1993).

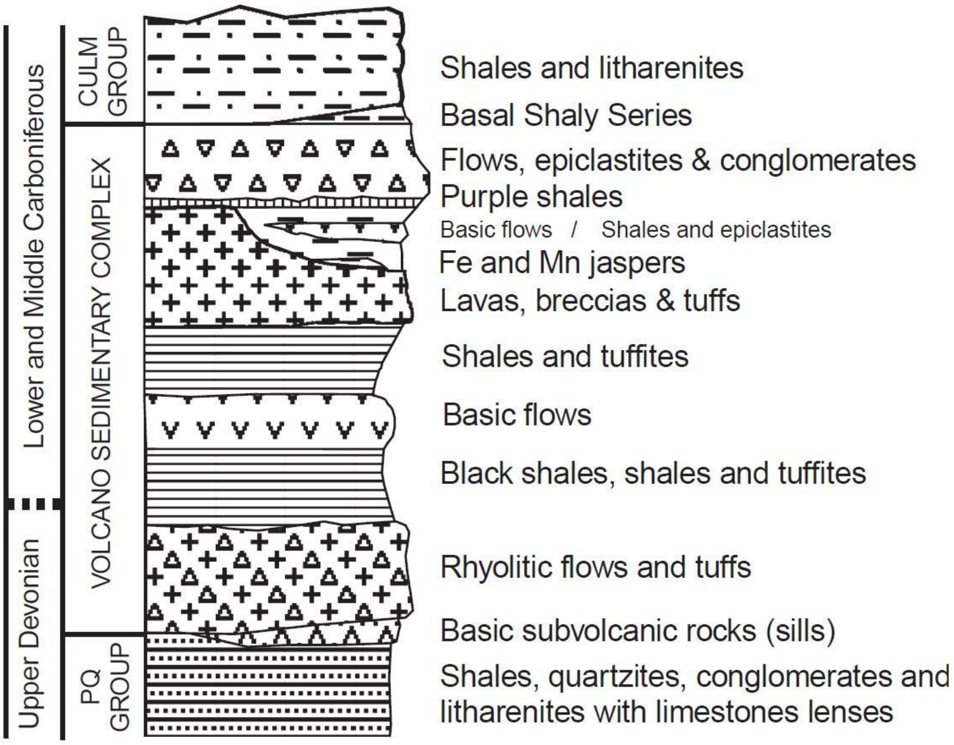

Figure 4.2. Generalized stratigrahphic column of the IPB (Ruiz de Almodóvar and Sáez, 1992).

Whole Belt is interpreted to be a tectonostratigraphic terrane sutured to the Iberian Massif during Variscan times (Quesada, 1991) as a thin-skinned foreland thrust and fold belt (Silva et al., 1990; Quesada, 1991). Tectonical history of the area was described by Sáez et al. (1999). Deformation resulted in asymmetric folds verging to SW, which often show transposed bedding on the short limb, producing structural features similar to those in a thrust belt. Three stages of deformation have been described in the Iberian Pyrite belt. D1 phase generated regional structures and low-grade regional metamorphism, whereas D2 and D3 slightly modified the D1 structures. Intensity of the deformation seem to increase from SW to NE (Schermerhorn, 1971; Ribeiro and Silva, 1983; Munhá, 1990). This tectonic event produced intense regional deformation which makes any detailed petrographic studies difficult. But the degree of metamorphism is very low (below lower greenschist facies).

Age of formation of the massive sulfide accumulations in the Iberian Pyrite Belt was estimated to be 350 Ma (near the Devonian/Carboniferous transition). It was defined by palynological studies (Pereira et al., 1996; Oliveira et al., 1997), U/Pb dating of hydrothermal zircons (Nesbitt et al., 1999), and Re/Os sulfide geochronology (Mathur et al., 1999; Nieto et al., 1999) and Rb/Sr geochronology (Relvas, 2000).

Massive sulfide deposits in the Iberian Pyrite Belt are stratigraphically associated with detrital and volcanoclastic horizons with significant ammount of black shales (e.g. Sáez et al., 1999). Accumulations of sulfide minerals occur in shapes of lenses or blankets. They show classical morphology and occur as stratiform massive bodies which are sometimes underlain by cross-cutting stringer zones, in which sulfides occur in veins or pervasive disseminations. But majority of the deposits are distal to the stockwork zone. Great abundance of re-sedimented, distal deposits is one of the characteristic of the Iberian Pyrite Belt (Schermerhorn 1970; Franklin et al. 1981). Mineral composition of the ores is characterized by relatively few major sulfide minerals. Most abundant sulfide mineral is pyrite followed by sphalerite, galena, chalcopyrite, tetrahedrite, arsenopyrite and pyrrhotite (e.g. Sáez et al., 1999). The most common minor mineral phases include Bi-Sb-Pb-As sulfosalts, stannite, cassiterite, magnetite, electrum, cobaltite (Ruiz de Almodóvar et al., 1994; Marcoux et al., 1996; Leistel et al., 1998; Almodóvar et al., 1998).

Hydrothermal alteration in the Iberian Pyrite Belt occurs at two different scales: (*i*) at a regional scale, where majority of the volcanic rocks are affected by a ‘hydrothermal metamorphism’ (Munhá and Kerrich, 1980) or ‘regional hydrothermal alteration’ (Barriga and Kerrich, 1984); (*ii*) and at a local scale, where strong hydrothermal alteration is related to the stockwork zones below the massive sulfide bodies. At a regional scale, alteration produced intense spilitazation of mafic and felsic rocks. In mafic rocks hydrothermal metamorphism produced chlorite, carbonates, epidote, albite and actinolite, involving extensive Na-K exchange, hydration, oxidation and carbonatization (Munhá, 1990). In felsic volcanics, the most common metasomatic processes were albitization, sericitization, chloritization and silicification (Munhá and Kerrich, 1980; Barriga and Kerrich, 1981, 1984; Barriga, 1983). This alteration processes required large amount of fluids from external reservoir, which was mainly the seawater.

Alteration connected with the massive sulfide accumulations is different. It is characterized by a concentric zonation, with chloritic zone in the middle and a peripheral sericitic zone (Carvalho 1976; Plimer and Carvalho, 1982; Barriga, 1983, Toscano et al., 1993; Ruiz de Almodóvar et al., 1994).

Mining in the Iberian Pyrite Belt has long history – from the pre-Roman times to present with only a few periods of inactivity (Pinedo Vara, 1963). During the last hundred years approximately 80 mines have been operating. In total they produced ~300 million tons of polymetallic ores, although sulfur and copper have been the main commodities processed in most cases (Strauss and Madel, 1974). With a few exceptions, the Iberian Pyrite Belt is not rich in gold. Average values are between 1.0 and 1.5 ppm (Leistel and Marcoux, 1995). Present mining activities are confined to five districts: Neves-Corvo (SOMINCOR) – Cu-Sn-Zn ores; Sotiel-Migollas (Almagrera S.A.) –Cu-Pb-Zn-S-Ag ores; Riotinto (Minas de Riotinto, S.A.L.) – Au-Ag ores; Aznalcóllar-Los Frailes (APIRSA-Boliden) – Zn-Cu-Pb-Ag ores; Tharsis (Minas de Tharsis, Caledonia) – pyrite and Au-Ag ores (Sáez et. al., 1999).

4.2. Representative ore deposits from the Iberian Pyrite Belt

4.2.1. Aljustrel deposit: Gavião ore body

The Aljustrel deposit is located in the Portuguese part of the Iberian Pyrite Belt. It consists of six orebodies: Estação, Feitais, Algares, Moinho, S. João, and Gavião (e.g. Schermerhorn and Stanton, 1969; Barriga 1983) located within an approximate area of 12 km^2. These ore bodies are situated on the top of the Aljustrel Volcanics, predominantly rhyolites and are overlain by metalliferous (Fe-Mn) sediments and jasper units (Fig. 4.3). The ore zone contains more than 200 Mt of massive sulfide ore with an average grade of 1 % Cu, 3.5 % Zn, 1.2 % Pb, 1 ppm Au, and 35 ppm Ag.

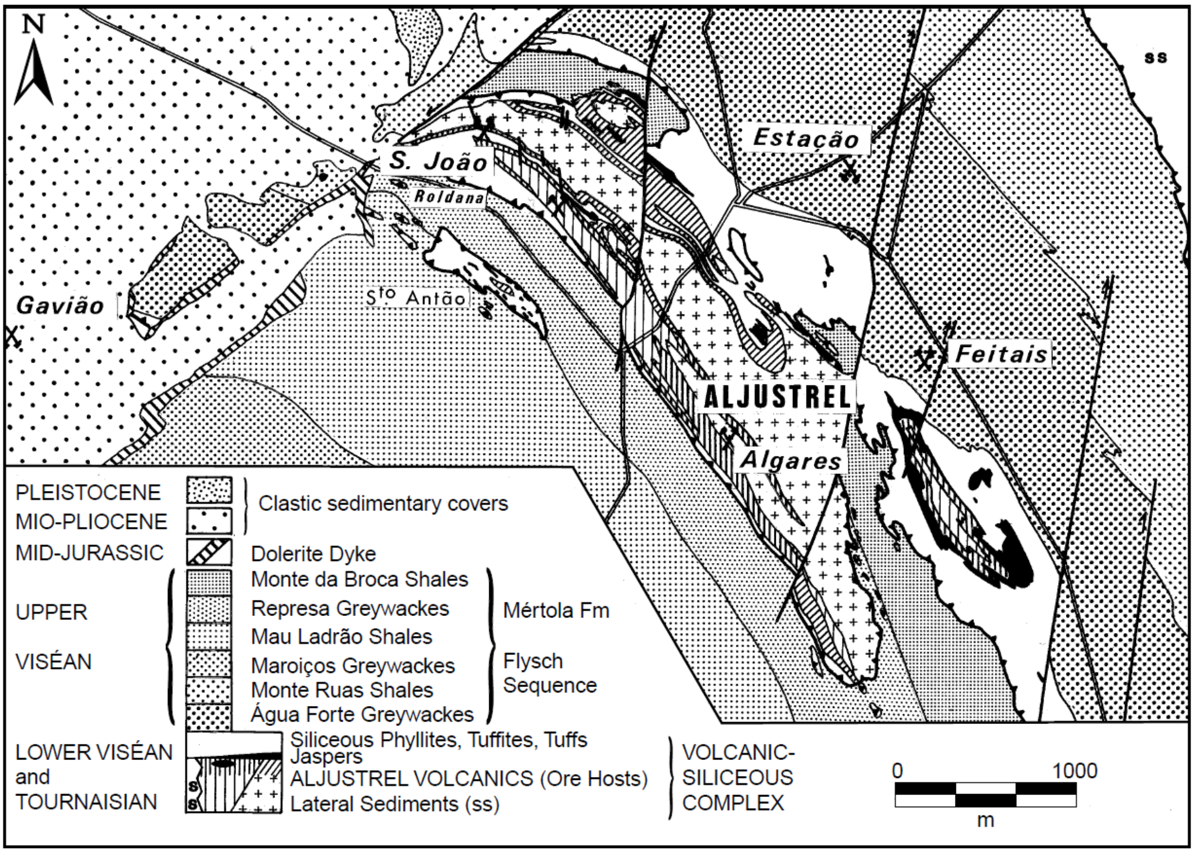

Figure 4.3. Geological map of the Aljustrel area (from Schermerhorn and Stanton, 1969; Andrade and Schermerhorn, 1971)

The ore bodies are hosted within the VSC sequence of the Aljustrel camp. This sequence consists of two major felsic volcanic units – the Quartz-eye Tuff and the Mine Tuff (Schermerhorn and Stanton, 1969). The quartz-eye tuff consists predominantly of porphyritic felsic volcanic rocks with quartz and feldspar phenocrysts set in a sericite-chlorite-carbonate-altered groundmass. The Mine tuff consists of volcaniclastic units devoid of quartz phenocrysts but locally hosts abundant sedimentary clasts. (Relvas et al., 2011). The volcanic sequence and massive sulfide bodies are overlain by jasper horizon (Paraíso Formation). This complex overlies the more recent lithologies belonging to the flysch group, an alternating sequence of schists and greywackes (upper Visean), along its SE border, which is marked by the major Aljustrel thrust fault (Oliveira, 1990).

The geological structure is folded and thrusted in a NW–SE direction and later cut by a series of NNE–SSW dextral strike-slip faults, events that took place during the different deformation phases of the Variscan orogenic cycle. The NW–SE striking lithologies have been offset by the left-handed strike-slip NW–SE, the Messejana Fault, a major structure that cuts across the crust and extends for hundreds of kilometers (Maia et al., 2012). Minor black shales from the host-rock succession of the Gavião ore bodies were dated to the Upper Tournaisian (ca. 350 Ma).Termination of the Aljustrel group is hidden under the Tertiary cover under which the two Gavião orebodies occur (Maia et al., 2012).

The Gavião ore bodies were described by Relvas et al. (2011): (*i*) the northeastern orebody is located within the reverse limb of the Central anticline and represents an extension of a mineralized zone developing to the south of the Messejana fault (as the S. João, Moinho and Algares orebodies). Northeastern orebody is tightly folded and disrupted by early thrust and wrench faults. It consisting of very low grade massive sulfiide ores (0.5 % Cu, 2.3 % Zn, 0.7 % Pb, 0.6 g/t Au, 18.8 g/t Ag); (*ii*) the southwestern orebody lies in the same stratigraphic position but it is situated in the reverse limb of the southwestern anticline. The orebody represents the highest average Cu grade within the whole Aljustrel camp (1.5 % Cu, 4.0 % Zn, 1.6 % Pb, 0.9 g/t Au, 48.3 g/t Ag).

The Gavião orebodies are interpreted to have formed in the proximity to complex volcanic center that consists of proximal facies of lavas and lava domes – clast-rotated hyaloclastites, and redeposited hyaloclastites – and possibly products of explosive eruptions (Relvas et al., 2011).

Mineral composition of the Gavião ores is very homogeneous; it major sulfide mineral is pyrite, minor minerals are sphalerite, chalcopyrite, arsenopyrite and tetrahedrite. Accessory mineral phases include galena, kobellite-tintinaite, stannite, pyrrhotite, boulangerite and bismuth (Relvas et al., 2011).

Alteration styles of the Gavião orebodies are spatially arranged into four zones (from the distal parts to the center): (*i*) distal albite zone characterized by weak sericitic alteration with sodium enrichment and hydrothermal quartz. Albite crystal are still present in this zone and primary textures are preserved (Fig. 4.4f, e); (*ii*) envelopes of the sericite alteration are subdivided into (*a*) less altered host rock with hydrothermal quartz veins (Fig. 4.4d) and rarely preserved feldspsar grains. Primary textures can be still sometimes recognized in this zone; (*b*) more intensively altered host rock with no original textures and structures preserved and prevailing sericite alteration. Minor sulfide minerals are disseminated in the altered mass (Figure 4.4c) or are present in a quartz veins. (Fig. 4.4b); *(iii)* chlorite center of the alteration zone. This part represents the core of the feeder zone – the stockwork. In this part volcanic rocks have been completely replaced by pervasive chloritic alteration (Fig. 4.4a) and veins with sulfide minerals and quartz. No original textures are preserved.

Sulfide mineralization of the Gavião ore body corresponds to a structure, which is characteristic for the majority of the volcanic-hosted massive sulfide deposits. The upper part of the massive sulfide body consists nearly exclusively of pyrite (Fig. 4.5a), and is almost barren with minor amounts of other sulfide minerals (chalcopyrite, sphalerite, and galena; Fig. 4.5b). Toward the foot wall, sphalerite starts to replace pyrite (Fig. 4.5c), and subsequently chalcopyrite penetrates the pyrite-sphalerite assemblage (Fig. 4.5d, e, f)

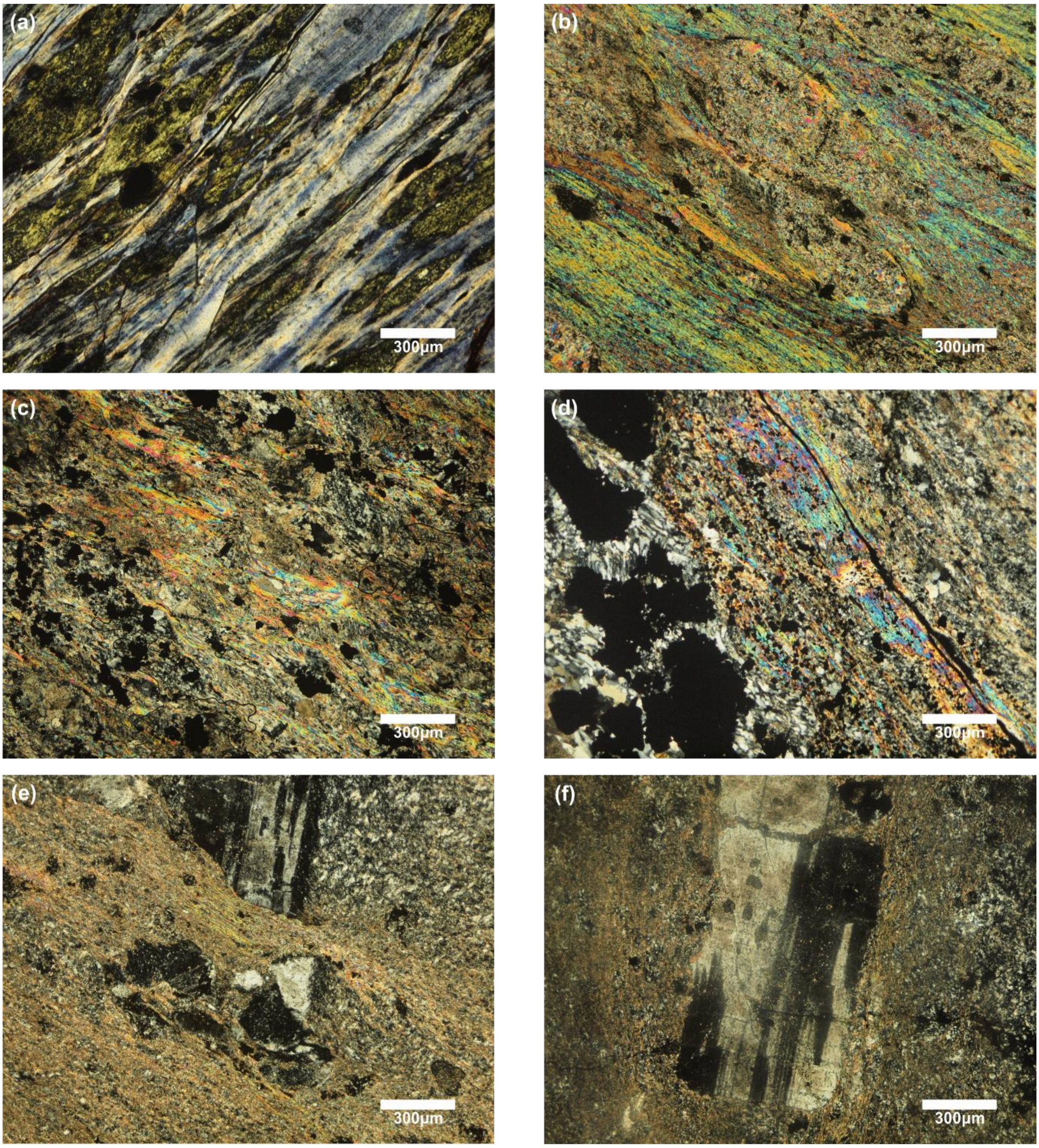

Fig. 4.4. Photomicrographs of hydrothermal alteration types of the footwall sequence of the Gavião ore body (drill hole SA 25): (a) intensely chloritized felsic volcanic rock; (b) intensely sericitized host rock; (c) intense sericitic alteration with abundant opaque minerals; (d) quartz vein with opaque minerals in intensely altered host rock. Small grains of opaque minerals are disseminated in the sericite-rich matrix as well; (e) partially preserved K-feldspar phenocrysts in a strongly sericitized rock matrix; (f) relic of plagioclase megacryst. This alteration type is distal to the core of the feeder zone.

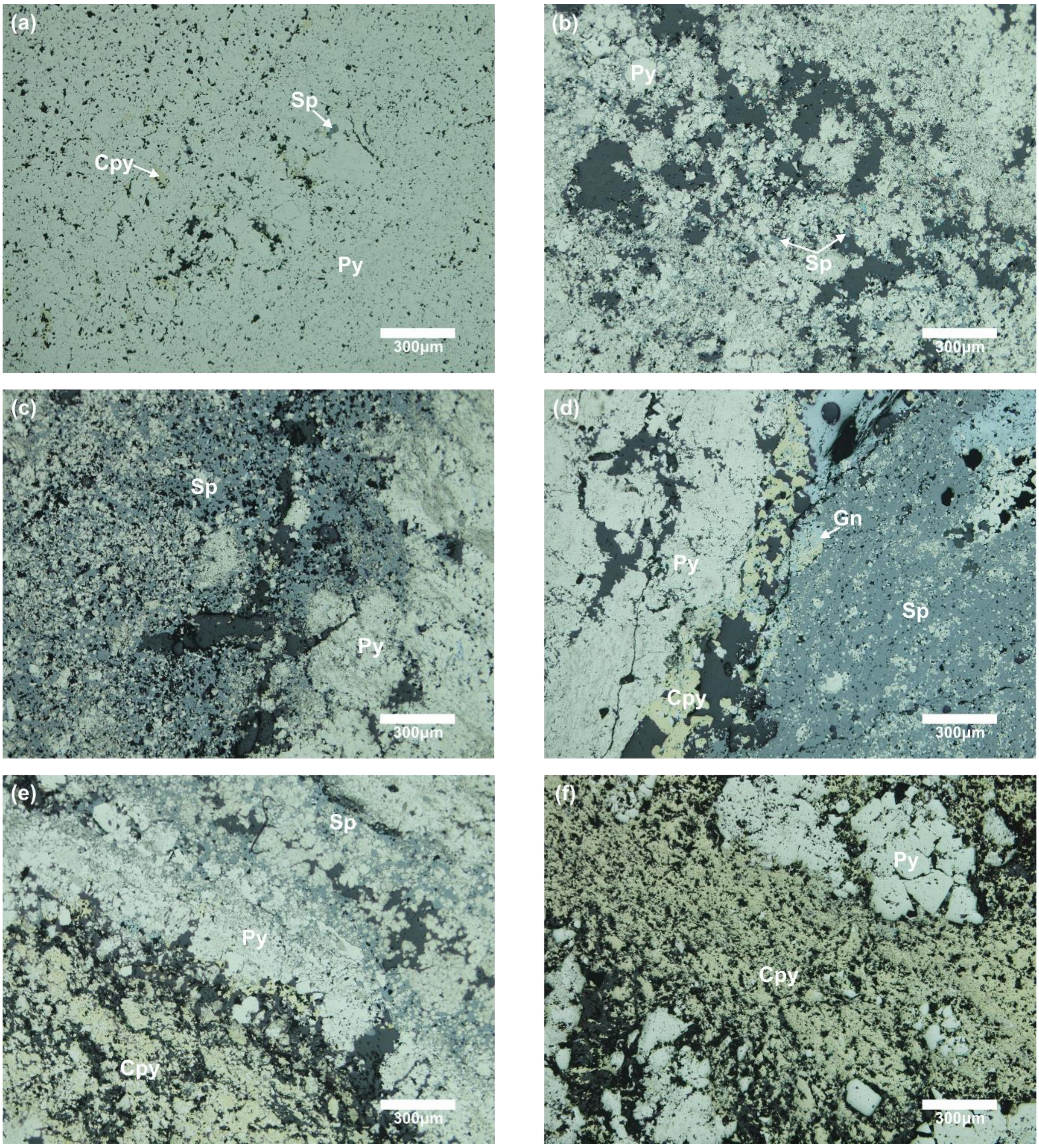

Plate 4.5. Photomicrographs of the sulfide ores from the Gavião ore body (drill hole SA 25): (a) massive pyrite from the top of the massive sulfide body. This sample is almost barren; minor phases include chalcopyrite, sphalerite, galena, and arsenopyrite; (b) massive pyrite affected by brittle deformation. Interstitial space, fractures, and cracks in pyrite are filled mostly by phylosilicates, sphalerite, and chalcopyrite; (c) replacement of early pyrite (to the right) by sphalerite (to the left). The sphalerite-rich replacement front incorporates incompletely replaced pyrite grains; (d) chalcopyrite veins penetrate the pyrite and sphalerite matrix. Significant amount of galena is present in this sample; (e) chalcopyrite is replacing pyrite, sphalerite and non-opaque minerals. Accessory minerals associated with chalcopyrite include galena and boulangerite; (f) prograding chalcopyrite invading and replacing pyrite. Mineral abbreviations: Py – pyrite, Cpy – chalcopyrite, Sp – sphalerite, Gn – galena.

4.2.2. Neves-Corvo deposit

The Neves-Corvo massive sulfide deposit is one of the largest (>300 Mt of ore) and richest VHMS deposits in the Iberian Pyrite Belt and in the world. It is located between the Messejana Fault and the Portuguese/Spanish border (Fig. 4.6). This deposit is unique due to its extremely high Cu and Sn ore grades (45 Mt at 6 % Cu, 4.5 Mt at 12 % Cu and 2.2 % Sn). More than 300,000 metric tons of tin metal is contained in several types of tin mineralization that grade from 500 ppm to 60 percent Sn (Relvas et al., 2006).

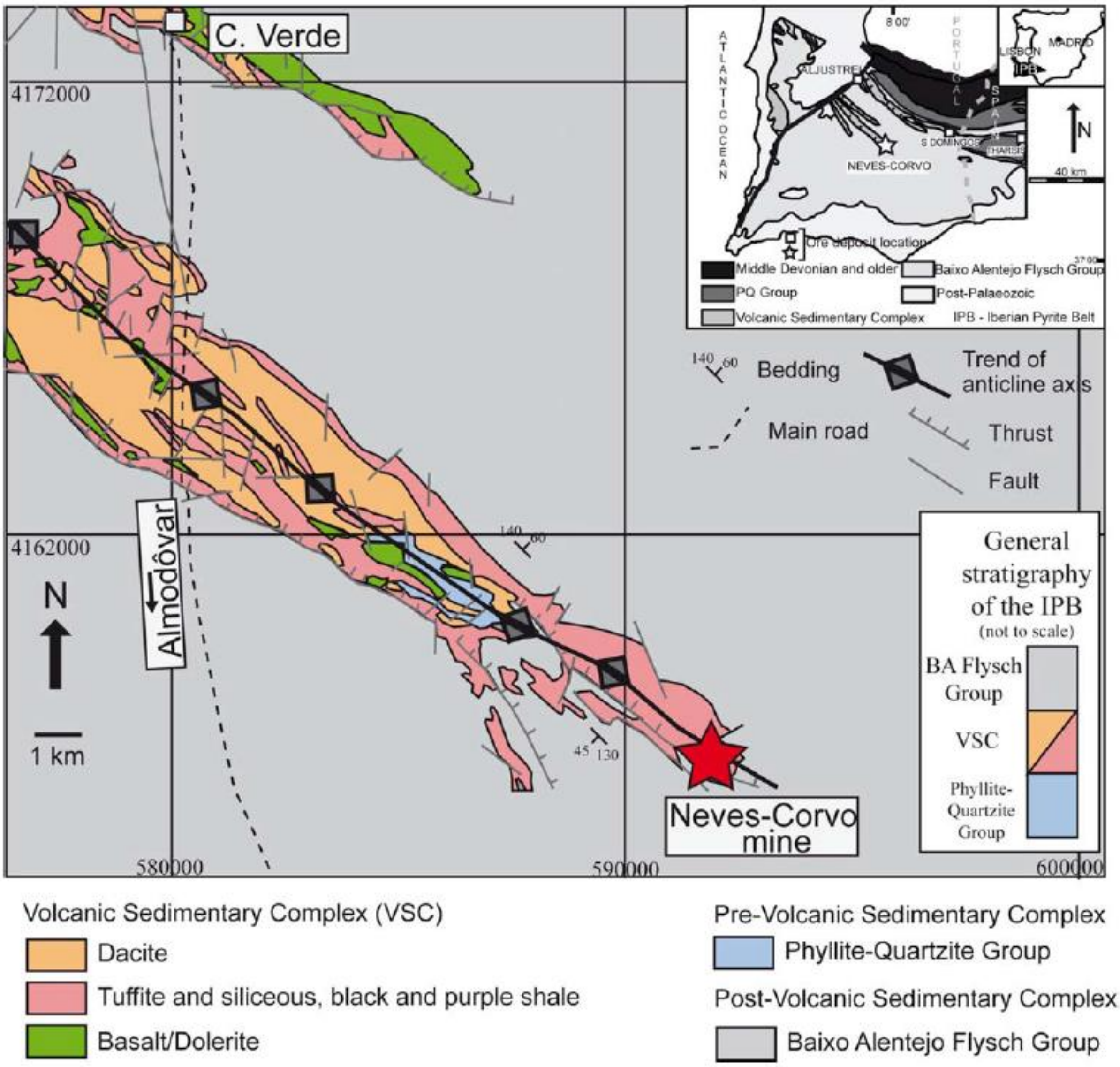

Fig. 4.6. Location of the Neves-Corvo Mine in the Rosário-Neves-Corvo antiform (adapted from Geological Map of Portugal, sheet 8, scale 1:200,000). Map shows location of the Iberian Pyrite Belt in the Iberian Peninsula and location of the Neves-Corvo Mine in the Iberian Pyrite Belt, (Thiéblemont et al., 1998)

The Neves-Corvo deposit consists from 6 orebodies – Neves, Corvo, Lombador, Zambujal, Graça and Semblana. Five orebodies were discovered in 1977 (Semblana in 2010) and exploitation was initiated in 1988. Exploration works still continue and as a result tonnage of the Neves-Corvo deposit is being continuously increased.

The Neves-Corvo ore bodies are hosted within a volcanosedimentary succession, which rests on a metasedimentary unit (Phyllite-Quartzite Group), and are overlain by a flysch sequence - Baixo-Alentejo Flysch Group (e.g. Relvas et al., 2006). This hanging-wall sequence is up to 900 meters thick. The rocks of the footwall sequence are predominantly coherent and consist mainly from the rhyolitic to rhyodacitic complex, fine grained volcanogenic sediments and dark shales (e. g. Relvas et al., 2006). The mineralization is hosted by this felsic complex, which was deformed into the Rosário-Neves-Corvo anticline complex (Fig. 4.7) which was formed at moderate water depth (below storm wave base) (e.g. Relvas et al., 2006). The Neves-Corvo deposit was dated ca. 350 Ma based on palynological and radiometric methods. This age corresponds to age of formation of majority of the deposits located in the Iberian Pyrite Belt.

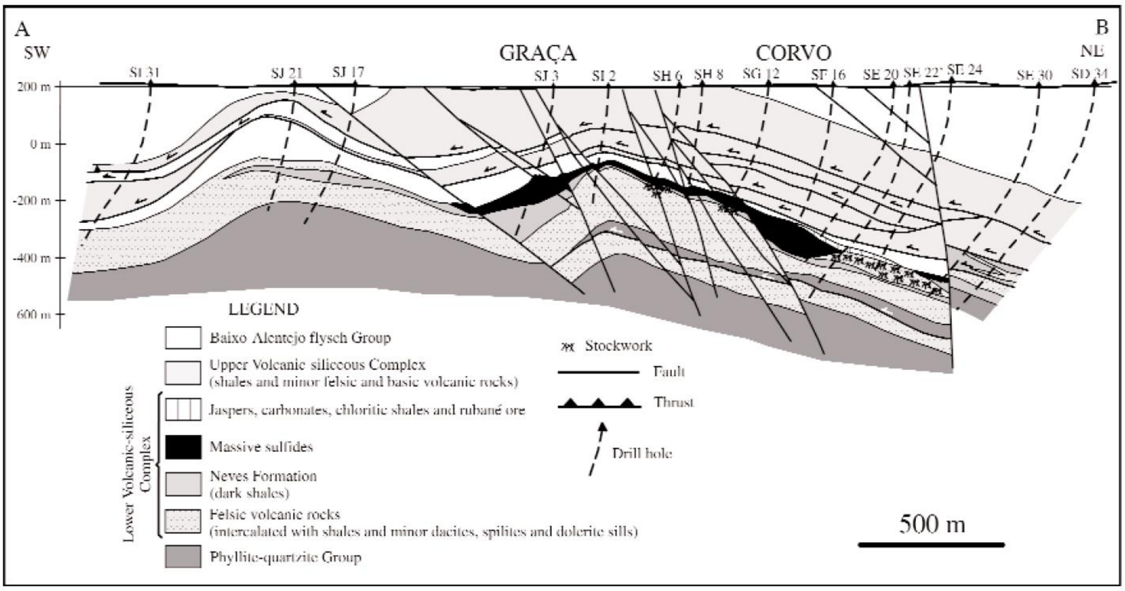

Figure 4.7. Geologic cross section through the Corvo and Graça orebodies (Relvas et al., 2006)

Composition and origin of the sulfide minerals at the Neves-Corvo deposit is unique compared to other deposits in the Iberian Pyrite Belt. The base metals distribution in the orebodies is a function of the syn-ore zone refining processes or as a function of post-ore tectono-metamorphic redistribution (fault-controlled ore-shoots) (Relvas et al., 2011). Due to the zone refining process (Figure 4.10.), massive sulfide bodies have typical ore zonation (copper on the base, pyrite on the top).

Hydrothermal alteration at the Neves-Corvo deposit shows the same patterns as at the Aljustrel deposit (Figure 4.4) and at the whole Iberian Pyrite Belt. At the Neves-Corvo deposit the Albite zone is not present due to enormous extent of the alteration system. Alteration zones can be subdivided into three zones (from the distal parts to the center): (*i*) envelope of the sericite alteration can be subdivided into (*a*) less altered host rock with hydrothermal quartz veins (Fig. 8b) and rarely preserved feldspsar grains. Primary textures can be still sometimes recognized in this zone; (*b*) more intensively altered host rock with no original textures and structures preserved and prevailing sericite alteration. Minor sulfide minerals are disseminated in the altered mass or are present in a quartz veins; *(ii)* chlorite center of the alteration zone. This part represents the core of the feeder zone – the stockwork. In this part volcanic rocks have been completely replaced by pervasive chloritic alteration and by veins with sulfide minerals and quartz. No original textures are preserved in the zone *ii*.

The massive sulfide ores are very variable and can be divided on the basis of their major sulfide mineral into: (i) chalcopyrite-rich ore (Fig. 4.8a, c, f); (ii) cassiterite- rich ores (Fig. 4.9a, b, c); (iii) sphalerite-rich ores. Majority of the ores are rich in chalcopyrite (Fig. 4.8) which is the main source of the copper. In some ores together with chalcopyrite, tetrahedrite is present as another source of Cu. Tin is present in the mineral cassiterite. Tin ores occur as a massive and stringer cassiterite ores or as the tin-rich, high-copper grade massive sulfide ore (Figure 4.9a). In the stringer cassiterite ores (Figure 4.9b) cassiterite is finely dispersed in the veins together with more abundant pyrite. One of the specific ores is the Rubané copper ore (Plate 4.8d) which consist mainly of pyrite and chalcopyrite. Due to the tectonic transportation this ore has “biscuit-cake” like tectonic fabric structure. It represents distal stockwork mineralization, which was tectonically emplaced on the top of the massive sulfide body (Corvo) (Relvas et al., 2006).

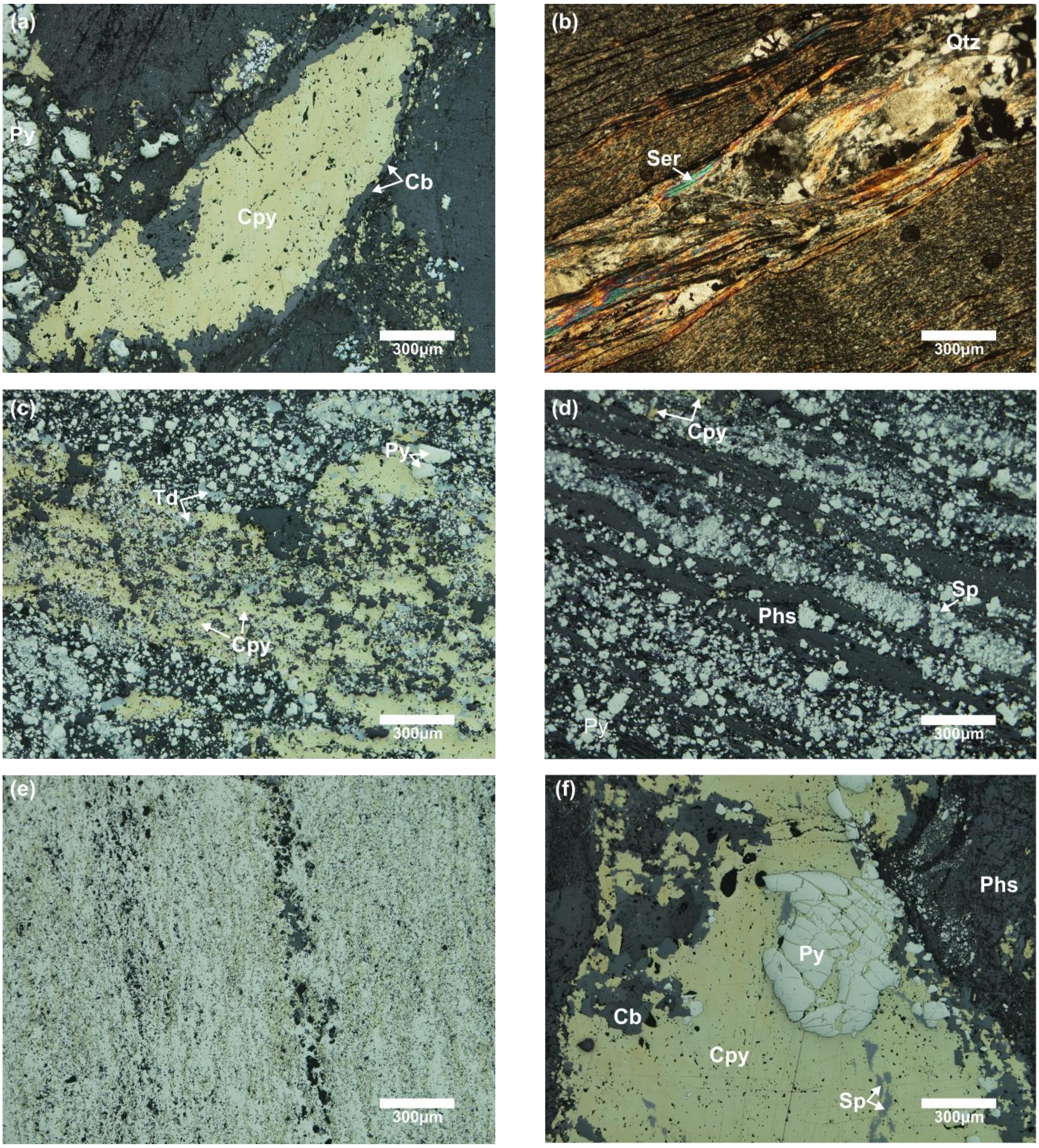

Fig. 4.8. Photomicrographs of various ore types from the Neves-Corvo deposit: (a) chalcopyrite grain with a carbonate ribbon and a residual pyrite in the altered host rock. Carbonates follow copper sulfides during remobilization and overgrows the chalcopyrite vein; (b) distal sericite-quartz vein in the altered host rock; (c) “rubané” tetrahedrite-chalcopyrite ore – the sample consists of partly recrystallized pyrite grain, with fissures in the pyrite grains; (d) “rubané” chalcopyrite ore. The banding resulted from tectonic transposition of the pyrite-sphalerite ± chalcopyrite stockwork veins; (e) massive chalcopyrite-pyrite ore. Pyrite has been replaced by chalcopyrite. Minor phases include sphalerite, stannite and cassiterite; (f) the relic grain of the pyrite was replaced by the chalcopyrite vein (with carbonate ribbon) together with sphalerite. Mineral abbreviations: Cb – carbonate, Cpy – chalcopyrite, Ser – sericite, Phs – phyllosilicates, Py – pyrite, Qtz – quartz, Sp – sphalerite, Td – tetrahedrite.

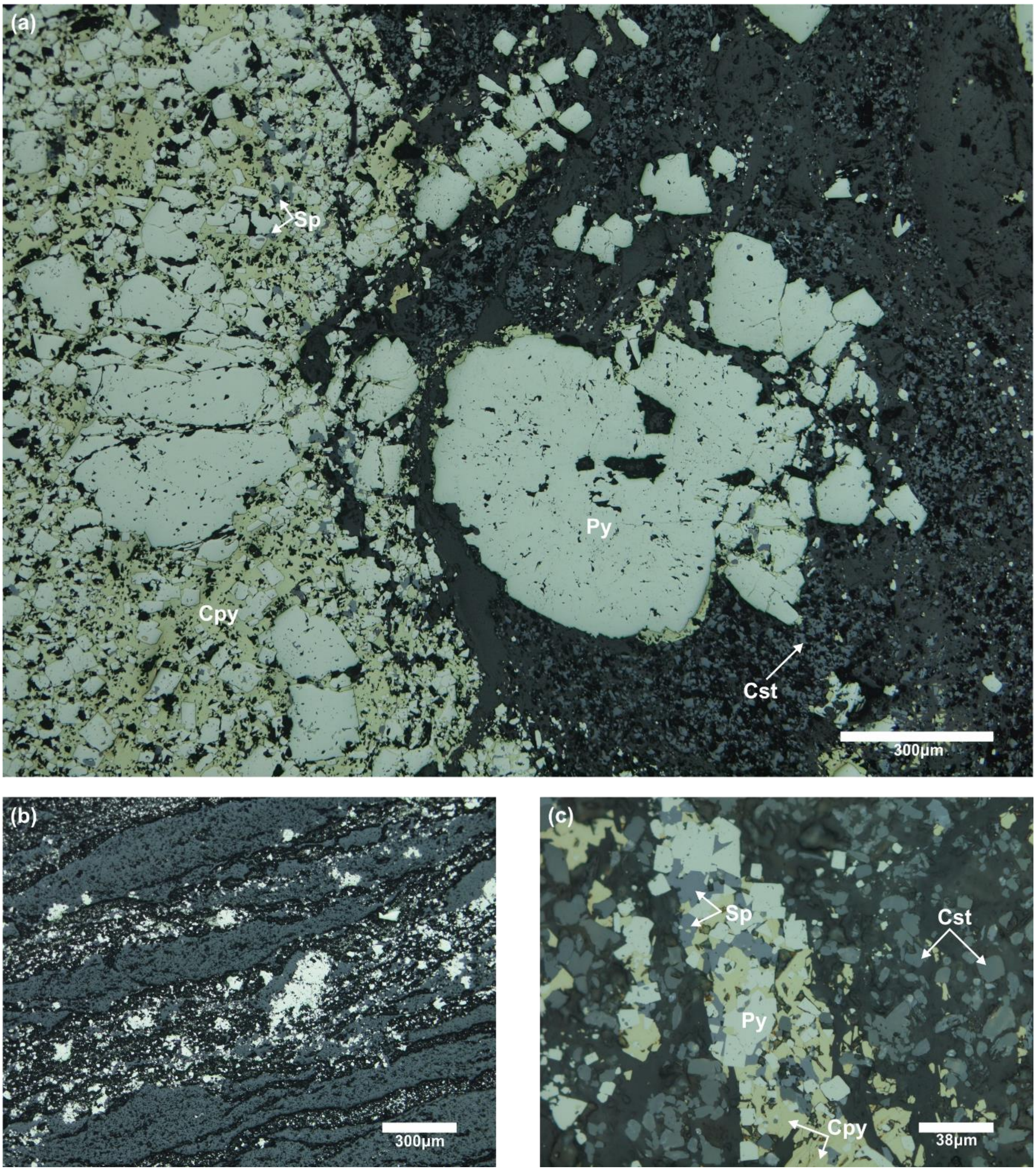

Fig. 4.9. Cassiterite ores from the Neves-Corvo deposit. (a) cassiterite-chalcopyrite ore with relics of pyrite. Chalcopyrite is accompanied by sphalerite; (b) veins that are filled with pyrite and small grains of cassiterite. Note the cataclastic deformation of pyrite; (c) detail of a sample in the photo a. A vein filled with pyrite, chalcopyrite and sphalerite which cuts the early stringer cassiterite ore. Mineral abbreviations: Cst – cassiterite, Cpy – chalcopyrite, Py – pyrite, Sp – sphalerite.

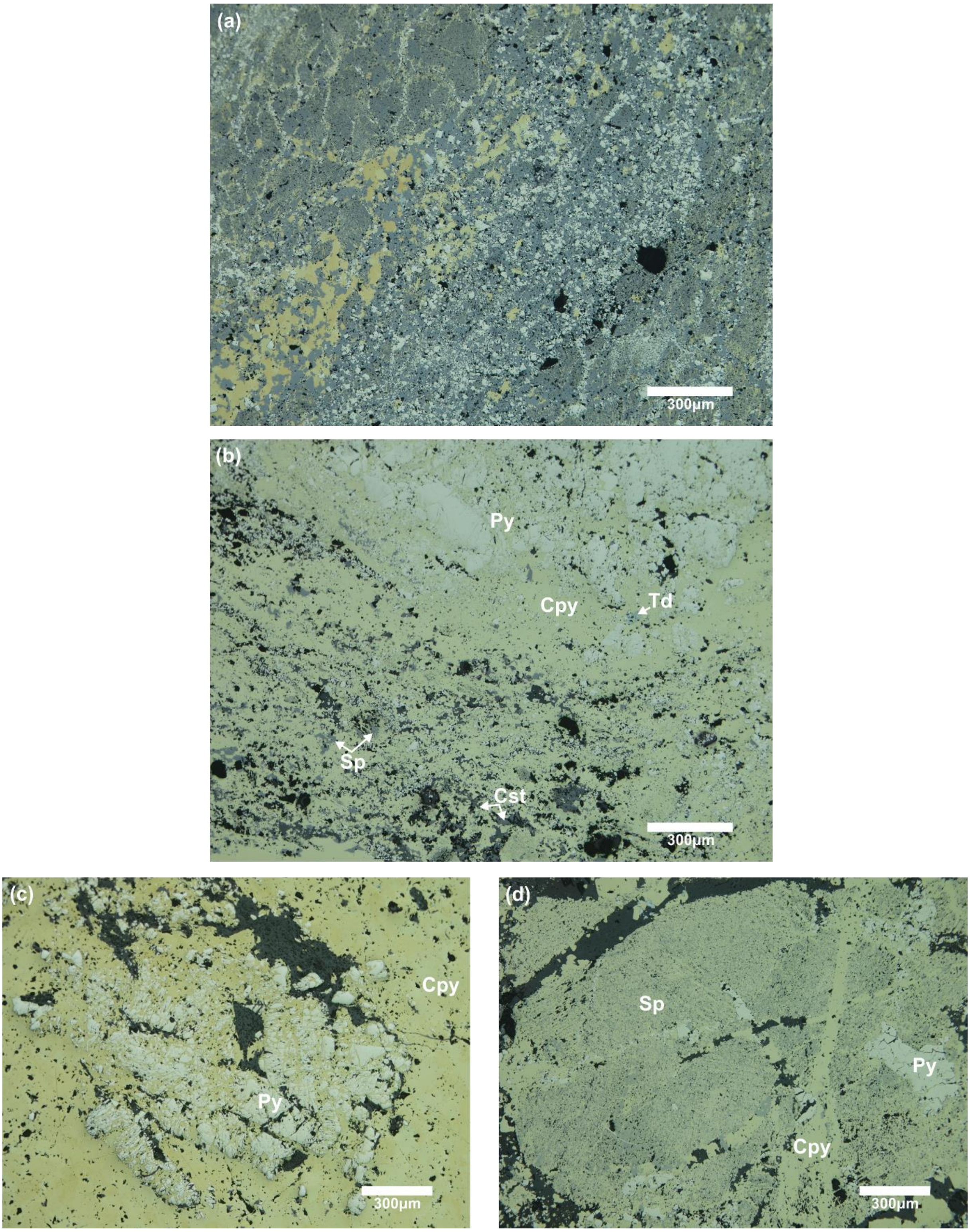

Plate 4.10. Different ore types from the Neves-Corvo deposit illustrate the zone refining process; (a) this ore situated on the top of the stockwork under the massive sulfide body. Chalcopyrite (and minor tetrahedrite) replaced sphalerite and early pyrite. Subsea-floor replacement of the volcanic rock was the main depositional mechanism in the Neves-Corvo deposit. This is evidenced by “relics” of the perlitic fracturing still preserved in some massive sulfide textures; (b) ongoing propagation of the chalcopyrite copper front led to almost complete replacement of the sphalerite (not all the sphalerite is flushed away from the system). Pyrite is more present due to its greater abundance. Cassiterite is also relatively abundant; (c) residual pyrite grain in a chalcopyrite mass. Brittle fracturing of pyrite and copper-enrichment due tectono-metamorphic remobilization are evidences of intense deformation; (d) relic grain of almost completely replaced sphalerite by chalcopyrite (same situation as in the picture b). Mineral abbreviations, Cst – cassiterite, Cpy – chalcopyrite, Py –pyrite, Sp – sphalerite.

5. Interpretation and Discussion

5.1. Iberian Pyrite Belt

The Iberian Pyrite Belt is a well-studied metallogenic district with extraordinary abundance of the volcanic-hosted massive sulfide deposits. By comparing of the Iberian Pyrite Belt with other deposits worldwide we can trace some specialties for which the Iberian Pyrite Belt is famous. On the following pages I will be describing main differences between the Aljustrel deposit and the Neves-Corvo deposit (Table 5.1).

Table 5.1. Comparison of the major features from the Aljustrel deposit and the Neves-Corvo deposit

Deposit	**Aljustrel**	**Neves-Corvo**
Alteration	classical alteration zoning – chlorite core, sericite envelopes and distal albite zone	the albite zone is not present due to enormous extent of the hydrothermal system
Mineralogy	mainly pyritic, sphalerite, chalcopyrite, arsenopyrite, tetrahedrite, galena	pyrite, chalcopyrite, sphalerite, tetrahedrite, cassiterite, stanite, bornite, arsenopyrite
Metal source	leaching metals from the Phyllite-Quartzite group	leaching metals from the PQ + magmatic fluid contribution (tin ores and bornite zone)
Genetic Model	long-lived hydrothermal system, low-sulfidation characteristics, no contribution from other metal source, classical ore zonation due to the zone refining process	long-lived hydrothermal system, low-sulfidation system with distinct high-sulfidation characteristics (bornite zones) due to the contribution of magmatic fluids and "extreme" zone refining process, occurrence of tin ores

5.2.1. Alteration and mineralization zoning

Footwall rock alteration of the rocks from the Iberian Pyrite Belt is characterized by a roughly concentric zonation, with an inner chloritic zone and a peripheral sericitic zone (Ruiz de Almodóvar et al., 1994). Albite zone is present only at some deposits. Mineralization and alteration styles in the Iberian Pyrite Belt occurred at moderate to low temperatures 350-70 ºC (Fig. 5.1), mildly acidic and low-sulfidation conditions (Relvas et al., 2009). Felsic magmatism provided the heat engine for convection and lateral migration of hydrothermal fluids and fault-controlled up flow and discharge of the circulating brines (Tornos et al., 2005).

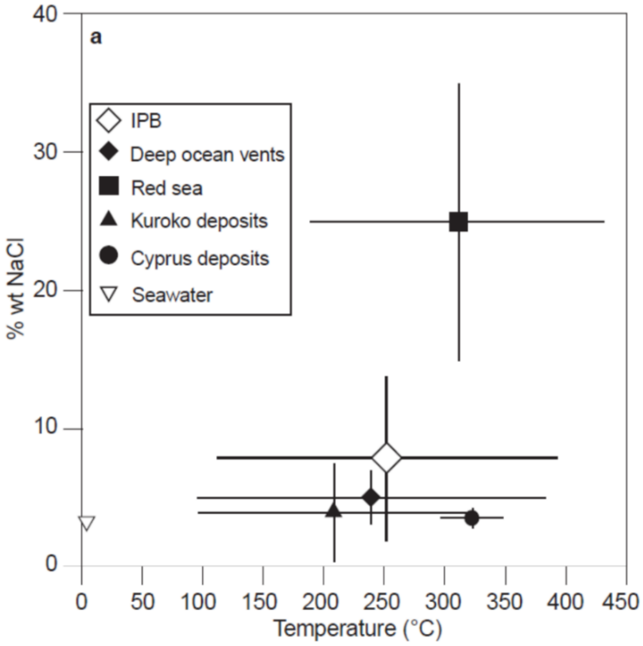

Figure 5.1. Temperature versus salinity diagram of primary inclusions from the Iberian Pyrite Belt compared with those in other reservoirs, mining districts and present-day vents (Sáez et al., 1999).

One of the newest model for the investigation of the temperature of formation using the chlorite composition was proposed by Lanari et al. (2014). This system is based on the Holland–Powell internally consistent thermodynamic data set. It uses the activity composition model for di-trioctahedral chlorite in the $FeO–MgO–Al_2O_3–SiO_2–H_2O$ system (Lanari et al., 2014). Sadly, I was unable to use this model, because it is made for chlorites with higher Al content than measured in Table. 5.3. But presumed temperature of formation of measured chlorite should corresponds with temperatures for inner stockwork chlorites given in the Fig. 5.2.

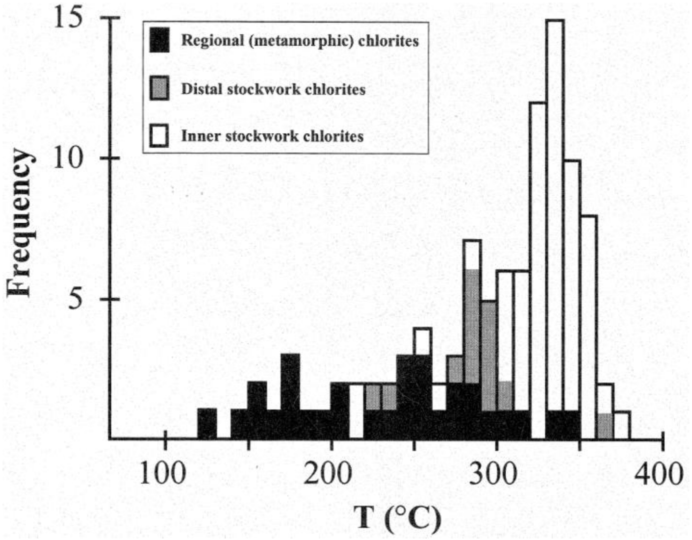

Figure 5.2. Histogram showing the range of the estimated crystallization temperatures for chlorites analyzed by Espana et al. (2000) using the Al^{iv} cation site occupancy method of Cathelineau (1988).

Mass-balance calculations by comparing altered and least-altered felsic volcanic rocks (by Espana et al., 2000) (Fig. 5.3) show that:

- Sericitization was accompanied by moderate enrichment in Mg, Fe and H2O, with depletion in Si, Na and K, and a slight net mass loss of about 3%.
- Chloritization shows an overall pattern which is similar to that of the sericitic alteration but with large gains in Fe, Mg and H_2O (and minor enrichment in Si, S and Mn), and a significant loss of Na and K and a minor loss of Ca and Rb.
- Chloritization involved much larger net mass change (mass gain of about 28%).

Primary mineralization from the deposits situated in the Iberian Pyrite Belt shows following textures (described by Sáez et al., 1999):

- Mineralization with no internal organization – ores of this type were deposited directly or very near of the hydrothermal feeder. They include mainly cupriferous and barren pyritic ores.
- Fragmental ores –common at the bottom of the of the sulfide masses. They consist mainly of sulfide fragments in a carbonated, siliceous or sulfide matrix. They are interpreted to be product of collapse or hydraulic brecciating (Lydon, 1988).
- Detrital ores – this ore type is characterized by preserved sedimentary structures including bedding and lamination. They have formed through transport and re-deposition of pyrite-rich muds (Routhier et al., 1978).

- Banded ores – characterized by bands of different main sulfide mineral. They are interpreted to be result of chemical precipitation far from the hydrothermal vents (García Palomero, 1980) or as the diagenetic banding.

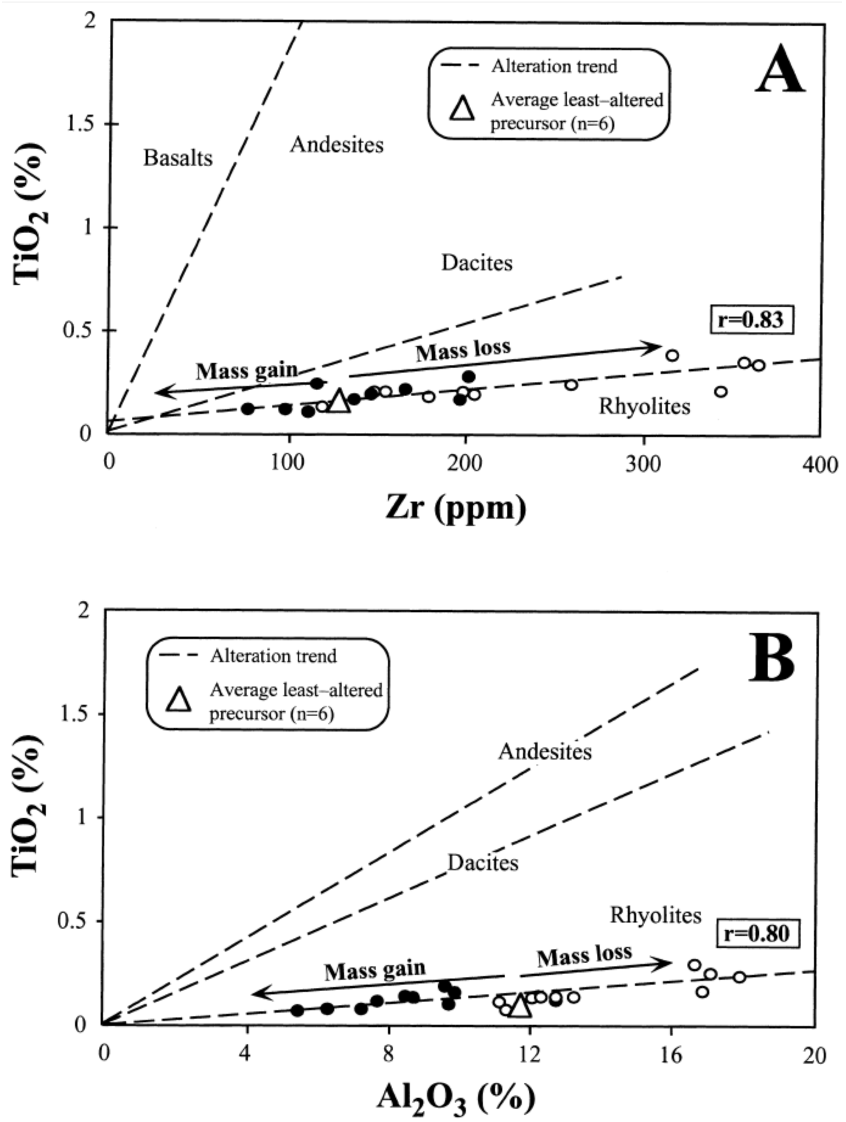

Fig. 5.3. Whole-rock geochemical variation diagrams for immobile constituents (Espana et al., 2000): (A) TiO_2 vs. Zr, and (B) TiO_2 vs. Al_2O_3 binary plots for the altered samples and average least-altered precursor. Symbols: *open circles* - sericitized rocks; *closed circles* - chloritized rocks. In both diagrams, a single alteration trend is obtained, thus indicating an initially homogeneous rhyolite unit (single precursor system with a constant ratio of immobile elements). Sericite-altered samples show substantial mass loss with respect to the least-altered precursor, whereas a net mass gain can be recognized in chlorite-altered rocks. The Pearson's product correlation coefficients (r) are greater than 0.8 in both cases. Reference dashed lines and volcanic rock fields after MacLean and Barrett (1993).

Both studied deposits share the same alteration patterns that are typical for the Iberian Pyrite Belt – chloritic alteration in the core of the alteration zone and envelopes of less and less intense sericitic-rich altered volcanic rocks. The albite zone is present only at the Aljustrel deposit, at the Neves-Corvo deposit is missing due to massive extent of the hydrothermal system. Stockwork is located the in the center of this alteration zone, which served as the pathway channel for hydrothermal fluids. The chlorite zone is characterized by an extreme leaching of Ca, Na and K and an enrichment in Al, Fe and Mg. The sericite zone is characterized by a leaching of Na and Ca which is accompanied by a significant enrichment in K and Al (Sáez et al., 1999). In the more distal zone of sericite alteration potassium and mainly sodium are being more abundant. Other metasomatic processes, including silicification, sulfidization and carbonatization, can also occur, related to one or both of these zones.

Mineralization zoning shares the same patterns at both studied deposits - top of the massive sulfide body consists almost exclusively of pyrite (barren). Bellow this zone, sphalerite and galena are present as the main economic sulfide minerals (pyrite, which is the main sulfide mineral is abundant in the whole body, but is not economic mineral). On the bottom, chalcopyrite-rich ores are situated. Chalcopyrite is also abundant on the top of the stockwork zone at the contact with the massive sulfide body. Distribution of sulfide minerals is a result of the zone refining processes.

5.1.2. Sericite and chlorite chemistry

Sericite and chlorite are the main alteration minerals and can be found in every alteration zone which is connected to mineralization in the Iberian Pyrite Belt. Chlorite is present due to intense hydrothermal processes in form of a pervasive alteration in the center of the alteration zone, besides sericite forms envelopes around the chlorite zone and represent less altered rocks. Chemical composition of these minerals can show relative proximity to the massive sulfide body. Analyzed sericite sample plotted into diagram showed muscovite composition (Fig. 5.4). Analyzed chlorite sample showed ripidolite composition (Fig. 5.5).

Mineral composition of alteration minerals, mainly of chlorite and sericite composition is being used as important exploration vector. The most generalized feature is a Fe±Mg enrichment and a Na±K depletion, in the proximity of the orebodies (Espana et al., 2000). Haloes with dispersed minerals with anomalous concentrations of elements, such as As, Tl, Ba, Sb or F, have been described by several authors (Schutz et al., 1988; Leistel et al., 1994). Toscano et al. (1993) and Leistel et al. (1994) have outlined the method of using the Fe/(Fe+Mg) ratio in chlorites, or the (Ba+K)/Na value in sericite, as potential tools in exploration for the massive sulfides.

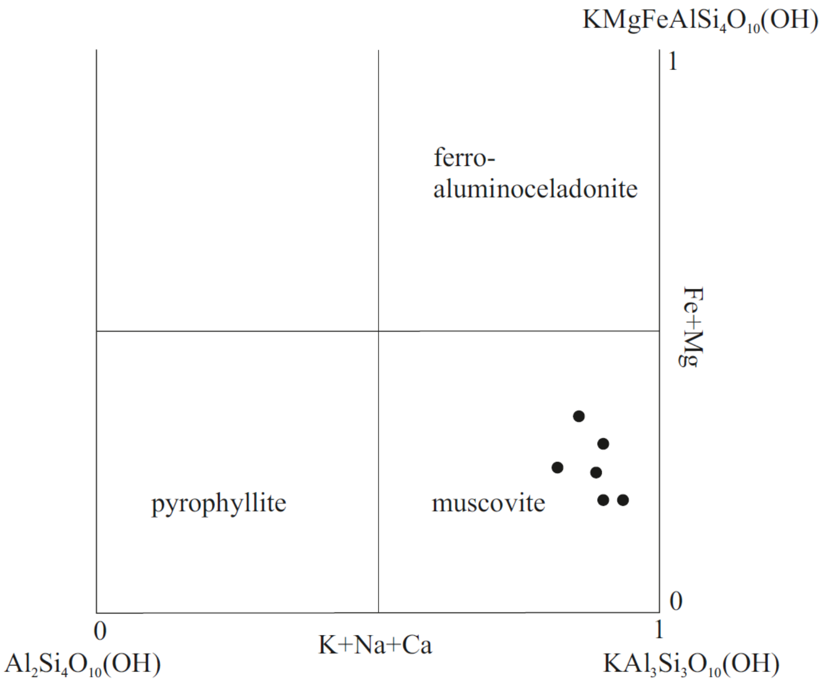

Figure 5.4. Chemical composition and classification of sericite from the Aljustrel deposit (graph by Rieder et al., 1998).

Table 5.2. Microprobe analysis of the sericite sample SA 25-564.4 from the Aljustrel deposit

Analysis	1	2	3	4	5	6
SiO_2 *(wt%)*	48.94	50.00	50.04	48.66	50.37	49.32
TiO_2	0.12	0.05	0.03	0.08	0.08	0.07
Al_2O3	32.95	31.43	30.23	33.05	30.34	32.11
Cr_2O_3	0.07	0.05	0.05	0.05	0.03	0,10
FeO	1.57	0.75	2.09	0.72	0.89	0.09
MnO	0.03	0.00	0.01	0.04	0.00	0.03
MgO	1.78	2.13	2.34	1.60	2.55	2.00
CaO	0.05	0.02	0.02	0.04	0.02	0.00
Na_2O	0.70	0.59	0.69	0.62	0.59	0.61
K_2O	8.70	9.59	9.04	9.67	9.78	10.09
F	0.47	0.53	0.72	0.38	0.44	0.58
BaO	0.47	0.19	0.18	0.36	0.19	0.23
H_2O	4.32	4.89	4.77	4.89	4.91	4.43
Total	100.17	100.20	100.21	100.15	100.16	99.65
Si *(per 11 O)*	3.23	3.31	3.33	3.23	3.34	3.28
Al (4)	0.77	0.69	0.67	0.77	0.66	0.72
Total	4.00	4.00	4.00	4.00	4.00	4.00
Al^{3+}	1.80	1.76	1.70	1.82	1.71	1,79
Fe^{2+}	0.09	0.04	0.12	0.04	0.05	0.00
Mn^{2+}	0.00	0.00	0.00	0.00	0.00	0.00
Mg^{2+}	0.17	0.21	0.23	0.16	0.25	0.20
Total	2.06	2.02	2.05	2.02	2.02	1.99
Ca^{2+}	0.00	0.00	0.00	0.00	0.00	0.00
Na^+	0.09	0.08	0.09	0.08	0.08	0.08
K^+	0.73	0.81	0.77	0.82	0.83	0.85
Total	0.82	0.89	0.86	0.90	0.90	0.93

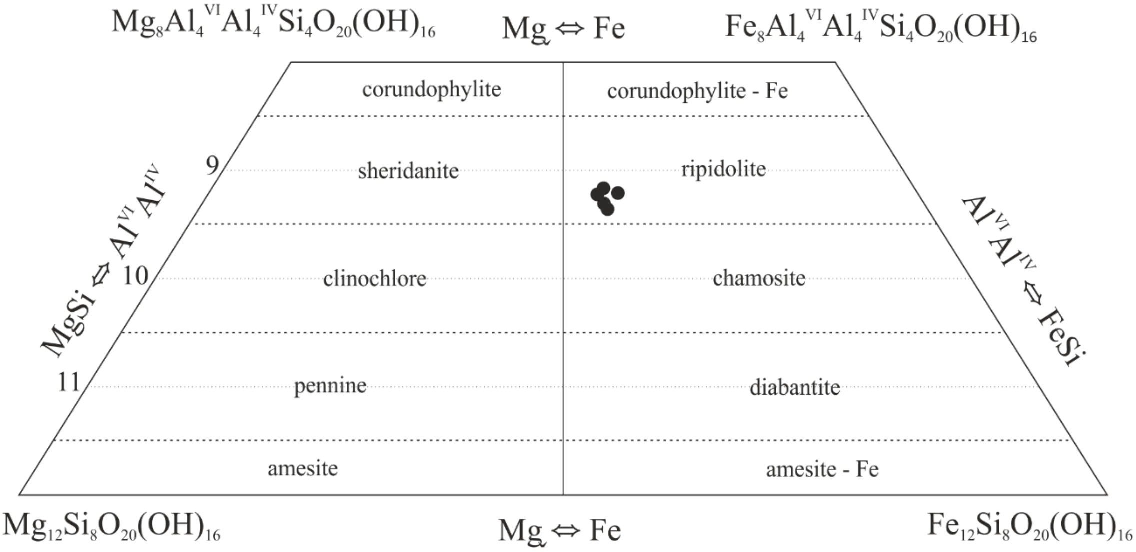

Figure 5.5. Chemical composition and classification of chlorite from the Aljustrel deposit (graph by Laird 1988).

Table 5.3. Microprobe analysis of the chlorite sample SA 25-263.3 from the Aljustrel deposit

Analysis	1	2	3	4	5
SiO_2 *(wt%)*	27.02	27.16	26.98	26.99	27.14
TiO_2	0.03	0.01	0.00	0.02	0.03
Al_2O3	20.85	20.64	20.96	20.86	20.63
Cr_2O_3	0.04	0.08	0.06	0.01	0.07
FeO	23.99	23.85	23.82	23.84	23.83
MnO	0.36	0.34	0.32	0.34	0.35
MgO	17.32	17.30	17.51	17.48	17.43
CaO	0.08	0.08	0.06	0.13	0.11
Na_2O	0.08	0.07	0.08	0.11	0.10
K_2O	0.01	0.01	0.02	0.01	0.01
H_2O	9.96	10.14	9.74	9.83	9.84
F	0.41	0.31	0.57	0.58	0.64
Total	99.74	99.68	99.55	99.62	99.54
Si *(per 28 O)*	5.50	5.54	5.49	5.49	5.53
Al (4)	2.50	2.46	2.51	2.51	2.47
Total	8.00	8.00	8.00	8.00	8.00
Al^{3+}	2.50	2.51	2.51	2.50	2.49
Fe^{2+}	4.08	4.07	4.05	4.06	4.06
Mn^{2+}	0.06	0.06	0.06	0.06	0.06
Mg^{2+}	5.25	5.26	5.31	5.30	5.29
Total	11.90	11.89	11.92	11.92	11.90
Ca^{2+}	0.08	0.06	0.06	0.06	0.06
Na^+	0.03	0.03	0.03	0.04	0.04
K^+	0.00	0.00	0.00	0.00	0.00
Total	0.11	0.09	0.09	0.11	0.10

5.1.3. Isotope geochemistry

Lead, strontium and neodymium isotope systematics suggest that most metals in the deposits located in the Iberian pyrite Belt should have been sourced by the, only partially known, sedimentary sequence (the Phyllite-Quartzite Group) that underlies the ore-hosting volcanic-siliceous complex (Marcoux, 1998).

At the Aljustrel deposit, the Phyllite-Quartzite group was the only source of metals, and it is consistent with prevalence of zinc than of copper both in the source and the ore body. Also the oxygen and hydrogen isotope data from the Aljustrel deposit include some of the highest $\delta^{18}O$ values ever recorded for volcanic rocks (Barriga and Kerrich 1984). They show that the Aljustrel volcanics were permeated and altered by sea water, shortly after their deposition and before the regional metamorphism and deformation (Barriga and Fyfe, 1998).

The sources of economic metals were traced using the radiogenic isotope composition of the Pb isotopes in the representative IPB ores and rocks (Fig. 5.6). Analyzed were sediments of the Phyllite-Quartzite Group (PQ) and sulfide ores of the “bornite zone” at the Neves-Corvo deposit. Jorge et al. (2007) propose this: the PQ rocks have lead isotopic compositions characterized by $^{206}Pb/^{204}Pb = 18.639 - 19.466$, $^{207}Pb/^{204}Pb = 15.639 -15.697$ and $^{208}Pb/^{204}Pb = 38.908 - 39.965$. The “bornite zone” ores expand the range of $^{206}Pb/^{204}Pb$ and $^{207}Pb/^{204}Pb$ values previously reported for Neves-Corvo ores, and form a steep linear trend in $^{206}Pb/^{204}Pb$ - $^{207}Pb/^{204}Pb$ space, independent from the one defined by cassiterite, with isotopic ratios varying from $^{206}Pb/^{204}Pb = 18.13$, $^{207}Pb/^{204}Pb = 15.59$ to $^{206}Pb/^{204}Pb = 18.43$, $^{207}Pb/^{204}Pb = 15.87$. Obtained data point to derivation of metals mainly from the Phyllite-Quartzite group (Jorge et al. 2007), which also predominates by volume in the stratigraphic sequence.

However, the sources for lead in “stringer and massive cassiterite” and “bornite zone” ores were distinct based on its Pb isotopic composition (e. g. Jorge et al., 2007). Observed variations in Pb isotopic compositions reflect ore-forming fluids with different origins and/or traveling along distinct hydrothermal pathways. They were equilibrated with rocks of different isotopic compositions, and finally mixed at the site of ore deposition (Jorge et al., 2007).

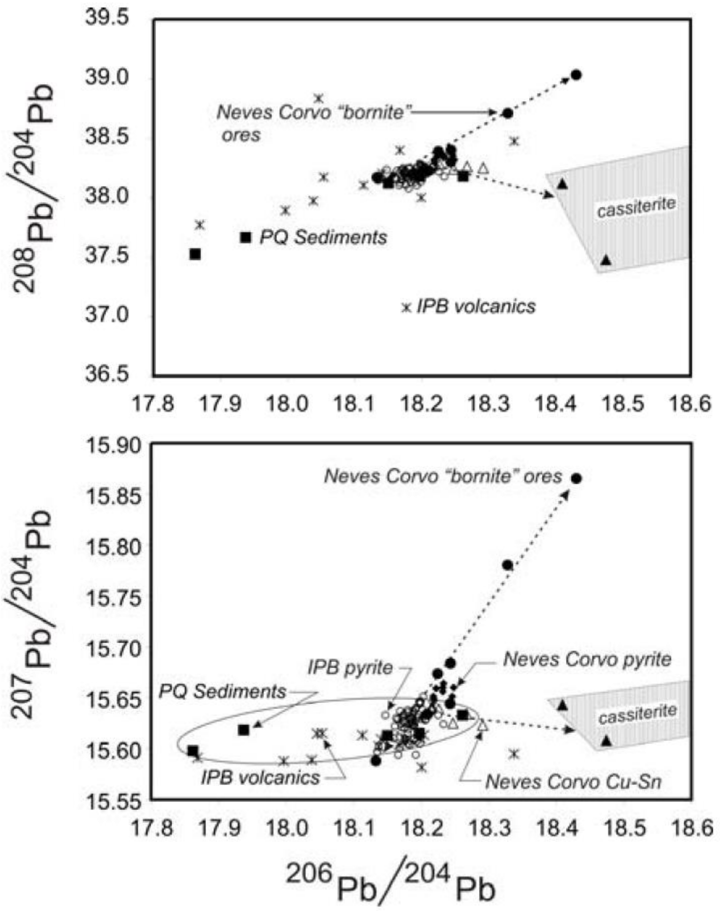

Figure 5.6. Diagrams of $^{206}Pb/^{204}Pb$ versus $^{208}Pb/^{204}Pb$ and $^{206}Pb/^{204}Pb$ versus $^{207}Pb/^{204}Pb$ for the Phyllite-Quartzite group and the IPB felsic volcanics, typical IPB ores, and the Neves-Corvo stringer and massive cassiterite, massive sulfide and "bornite zone" ores (Jorge et al., 2009).

Nevertheless, in some deposits (e.g. Neves-Corvo) there is a strong evidence for a contribution of magmatic fluids with metals from a different source. This fluids were rich not only in copper but also in tin which lead to creation of massive and stringer cassiterite ores. Additional copper-rich fluids and "extreme" zone refining process created the "bornite zone" where copper grades are up to 44.1%. Only similar deposit in terms of mineralogical composition is the Kid-Creek in Ontario, Canada. The mineralogical, geochemical, and oxygen and hydrogen isotope characteristics of hydrothermally altered rocks at Neves-Corvo indicate that the ore fluids were hotter and more acidic than typical ore-forming fluids of the IPB (Relvas et al., 2006). The temperature is interpreted to be ~380ºC.

The "bornite zone", where copper grades are up to 44.1% is one of the results of magmatic fluid contribution into the VHMS system. Ore mineralogy of the "bornite zone" displays typical high-sulfidation characteristics (the presence of bornite, tennantite, mawsonite, stannite, miharaite, carrolite, stromeyerite, wittichinite) in prevailing low-sulfidation system (Relvas et al., 2009). Gold content in this zone is also very high (up to 94.5 ppm Au). The elemental suite that accompanies gold is Bi, As, Co, Cu, Sn, In, Hg, Te, Se and Sb (Pinto et al., 2005). This zone is a result of both the extreme zone refining process and the late magmatic fluid input, which was the source of "extra" copper, (e. g. Relvas et al., 2009). This copper was not possible to be leached from the PQ group, which points to the magmatic-fluid contribution.

Another result are the massive and stringer tin ores. Tin occurs as cassiterite, stannite which is similar to the Cu-Sn paragenesis at the South orebody of the Kidd Creek deposit (Hannington et al., 1999). Lead, Os and Nd isotopic signatures of the "stringer and massive cassiterite ores" are comparable to those for granite-affiliated cassiterites and indicate external sources (Relvas et al., 2001; Munhá et al., 2005). This unusual ore is interpreted to be a result of a late magmatic-fluid input into the VHMS system derived probably from the hidden tin-enriched granitods.

5.1.4. Genetic model of the Iberian Pyrite Belt

The Iberian Pyrite Belt forms a metallogenic province developed in a rather spatially restricted and relatively thin (<600 m) (Jorge et al., 2007) volcanic sequence deposited in a pull-apart basin of transpressive orogen (Tornos, 2006). Leaching metals from the footwall sequence (Phyllite-Quartzite group and its unknown basement) and the minor felsic volcanic rocks was the main source for the metal supply in the typical IPB deposit. Felsic magmatism and connected high heat flow were the main driving forces for convective circulation of the sea water, leaching and dewatering of siliciclastic sediments of the Phyllite-Quartzite group (Fig. 5.7). The hydrothermal fluids were channeled along regional faults and deformation zones.

The massive sulfides were formed in two main different settings (described by Tornos, 2006): as exhalative ores in brine pools on the sea bottom, or as replacement-style mineralization well below the seafloor (Fig. 5.7). They show a classical VHMS morphology, occurring as stratiform bodies underlain by cross-cutting stringer zones, in which sulfides occur in veins or are pervasively disseminated. Most of the orebodies have formed in a relatively short time period during the uppermost Devonian by the exhalation of deep connate brines into third order basins. These accumulations are hosted mainly within shales. For the replacive ores there is no time constrain for the time of formation, they have been forming in at least three separated horizons of the Volcanic Sedimentary Complex. The replacive ores are restricted to layers with high primary permeability within the felsic volcanic sequence, including glass-rich and pumice-rich felsic volcaniclastic sediments. Products of this process are the stratabound orebodies that probably did not have hydrothermal expression on the seafloor.

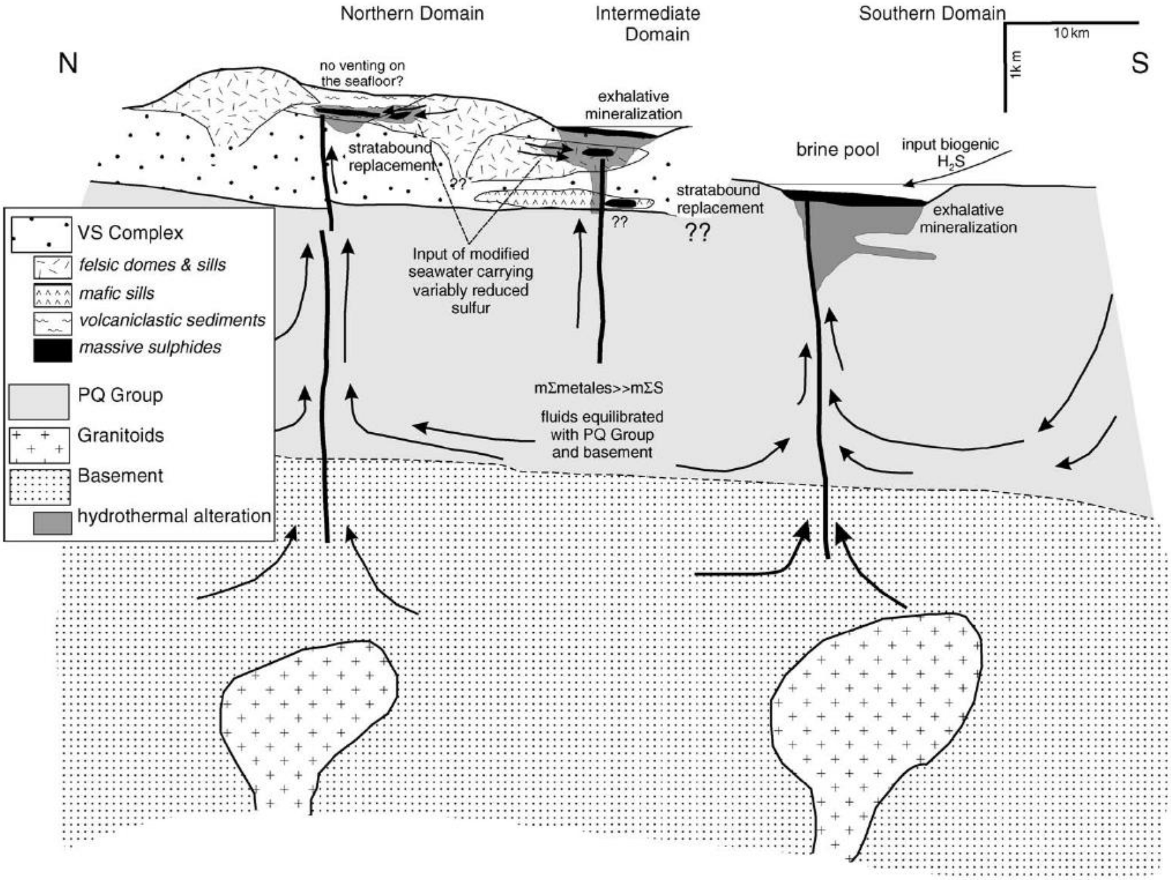

Figure 5.7. Conceptual model of formation of the massive sulfide bodies in the Iberian Pyrite Belt with hypothesized granitoid bodies involved (Tornos, 2006).

Larger deposits (>100 Mt of ore) are estimated to be results of long lived hydrothermal system. Nascent bodies and structures where then affected and modified by Variscan deformation (Tornos, 2006). Conclusions of this deformation were described by Tornos (2006). The thrusting and folding had several major effects including:

- Displacement of the massive sulfide bodies away from the stockworks and their present location in regional tectonic ramps (Quesada, 1998). Also syn-sedimentary faults were tectonically inverted.
- Massive sulfide lenses were tectonically stacked in a ramp which led to creation of flat morphology and increase in their overall thickness (Aznalcóllar, Almodóvar et al., 1998; Tharsis, Tornos et al., 1998).
- Massive sulfide lenses were also dismembered and flattened which led to significant changes in their original aspect ratio.
- Significant enrichment in gold along deformation bands (Tornos et al., 1998) and in copper in the stockwork zones (Gumiel et al., 2001). There is also enrichment in the

base metals and gold in the more deformed zones of the massive sulfide bodies (Velasco et al., 2000; McKee et al., 2001).

- Syn-tectonic pyrite-rich stockworks were formed without related hydrothermal alteration (Tornos et al., 1997).

Why the Iberian Pyrite Belt hosts extraordinary density of the massive sulfide accumulations compared with other mining districts is still not clear and requires further research.

5.2. Volcanic-hosted massive sulfide deposits in the World

5.2.1. Origin of alteration and mineralization zoning

Alteration zones result from reaction between the seawater (modified into hydrothermal fluid) and volcanic rocks (Fig. 5.8). Temperature of the fluids is estimated to vary from 200ºC to 350ºC (based on the fluid inclusion evidence from Pisutha-Arnond and Ohmoto, 1983; Khin Zaw et al., 1996). Fluids are also mildly acidic. Water/rock ratio is estimated to be between ≈5 to > 100 (Barrett and MacLean, 1994).

Barrett and MacLean (1994) also described main chemical changes, which occur at high water/rock ratio:

- Leaching of Na and Ca which leads to change of albite and other feldspar components into sericite and chlorite.
- When CO_2 is present in the system it leads to the formation of calcite. Actinolite phases are not stable a do not form. If epidote is formed it is then destroyed with increasing alteration intensity.
- By dissolution of Fe and Ca-Si, ilmenite ($FeTiO_3$) and sphene ($CaTiSiO_5$) are degraded into rutile (TiO_2).

Key process connected with the creation of alteration zones around the VHMS deposit is the primary feldspar destruction and creation of sericite and chlorite:

$3\ NaAlSi_3O_8$ (feldspars, mainly albite) + $K^+ + 2\ H^+ =$
$KAl_3Si_3O_{10}(OH)_2$ (sericite) + $6\ SiO_2$ (quartz) + $3\ Na,^+$ (5.1)

$2\ KAl_3Si_3O_{10}(OH)_2$ (sericite) + $3\ H_4SiO_4$ (aq, quartz) + $9\ Fe_2^+ + 6\ Mg_2^+ + 18\ H_2O =$
$3\ Mg_2Fe_3Al_2Si_3O10(OH)_8$ (chlorite) + $2\ K^+ + 28\ H.^+$ (5.2)

The first reaction represents sericite replacement of albite in the outer parts of the alteration system, and the second is common closer proximity to a massive sulfide mineralization, where chlorite-rich assemblages are dominant (Large et al., 2001). Reaction 5.1 involves a loss of Na_2O (and CaO) and a gain of K_2O, whereas reaction 5.2 involves a loss of K_2O and gain in FeO and MgO, on the basis of constant Al_2O_3 (Large et al., 2001).

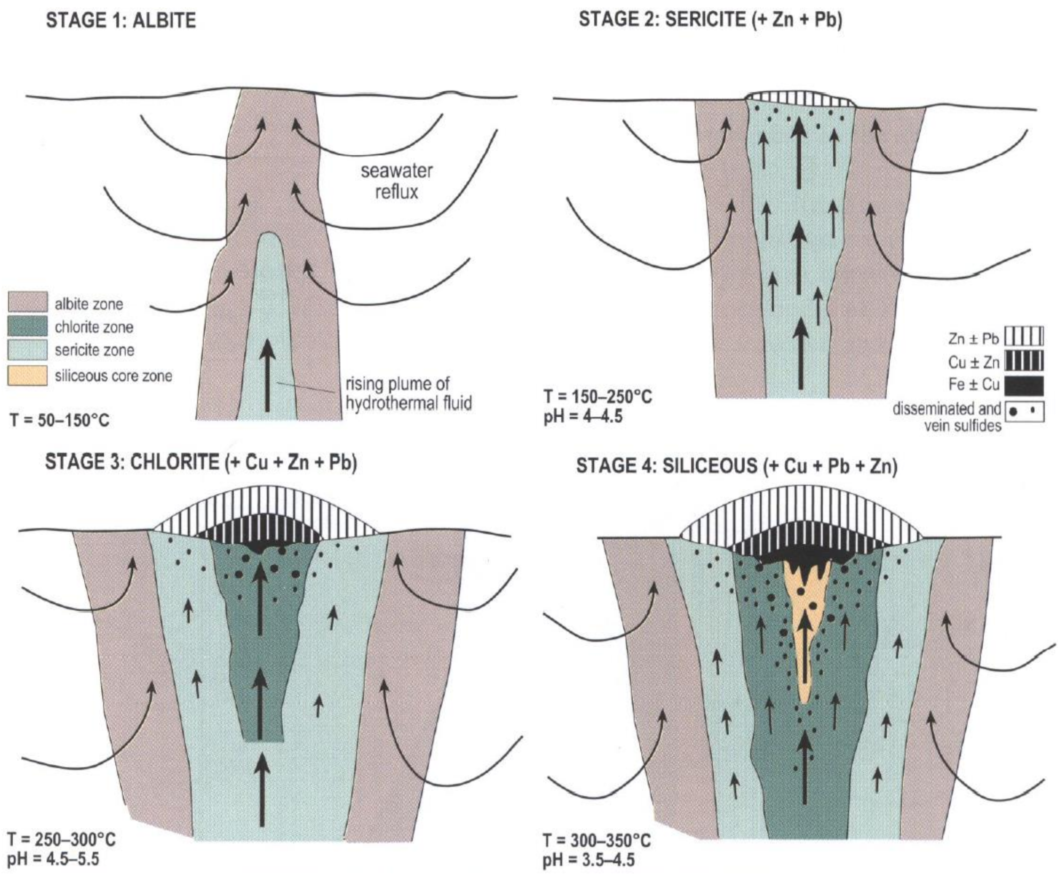

Figure 5.8. Model of creation of the footwall alteration zoning in a mound-style massive sulfide deposit. Solomon and Groves, (1994) and Solomon and Quesada, (2003) divided this process into four stages. First stage represents low-temperature system which produced the albite zone. At the second stage due to increase in temperature sericite and Zn – Pb rich-sulfide zones develop. Copper is for the first time present in the third stage due to higher temperature (250 ºC - 300 ºC). At the fourth stage, maximum temperature and low pH result in siliceous core zone and Cu + Pb + Zn sulfide-rich zone.

Large et al. (2001) divided main alteration trends connected with the volcanic-hosted massive sulfide deposits into hydrothermal trends (Fig. 5.9a) and diagenetic trends (Fig. 5.9b) situated in the alteration box plot. The alteration box plot is a plot of the AI (Alteration Index) versus the CCPI (Chlorite-Carbonate-Pyrite Index)."Least-altered boxes" are determined either through petrographic investigations in cases where the sample material is relatively fresh and unaltered, or as shown in Fig. 5.9, where the least-altered box was selected based on previous work with similar (e.g. basalts, andesites, dacites and rhyolites), but variously altered rock types. The alteration index (*AI*) is calculated in the following way:

$$AI = \frac{100(K_2O + MgO)}{(K_2O + MgO + Na_2O + CaO)}, \qquad (5.3)$$

This is often referred to as the Ishikawa alteration index defined by Ishikawa et al. (1976). It measures the degree of the breakdown of the Na-plagioclase and volcanic glass and subsequent replacement by sericite and chlorite. Second index is called the chlorite-carbonate-pyrite index (*CCPI*):

$$CCPI = \frac{100(MgO + FeO)}{(MgO + FeO + Na_2O + K_2O)}, \tag{5.4}$$

FeO represents total (FeO + Fe_2O_3) content of the rock. Mg-Fe chlorite alteration is typically developed close to VHMS deposits where hydrothermal temperatures and water/rock ratios are at their maximum (Large et al., 2001). The *CCPI* index has been designed to measure the increase in MgO and FeO associated with the Mg-Fe chlorite development. Chlorite commonly replaces albite, K feldspar, or sericite in the volcanic rock, leading to a loss of Na_2O and K_2O such it is described in the equation (5.2) (Large et al., 2001).

Hydrothermal trends (Fig. 5.9a) include:

- Weak sericite alteration at the margin of a hydrothermal system in a felsic volcanic host rocks.
- Intense sericite-chlorite ± pyrite alteration typically found in the footwall of a VMSD within both felsic and mafic volcanic.
- Chlorite ± sericite ± pyrite alteration is typically found in the chlorite-dominated footwall in both felsic and mafic volcanic rocks.
- Chlorite-carbonate alteration typically developed in immediately adjacent to massive sulfide lenses.
- Sericite-carbonate alteration which is found in the immediate hanging wall to a massive sulfide mineralization.
- K-feldspar-sericite, an uncommon trend occasionally seen in the footwall in a felsic volcanic rocks.

Diagenetic trends include (Fig. 5.9b):

- Albite-chlorite, typical of seawater interaction at low temperatures (e.g. spilitization).
- Epidote-calcite ± albite which is a common alteration trend found in intermediate to mafic volcanic rocks.
- K-feldspar-albite, an early diagenetic trend of K-feldspar replacing albite.

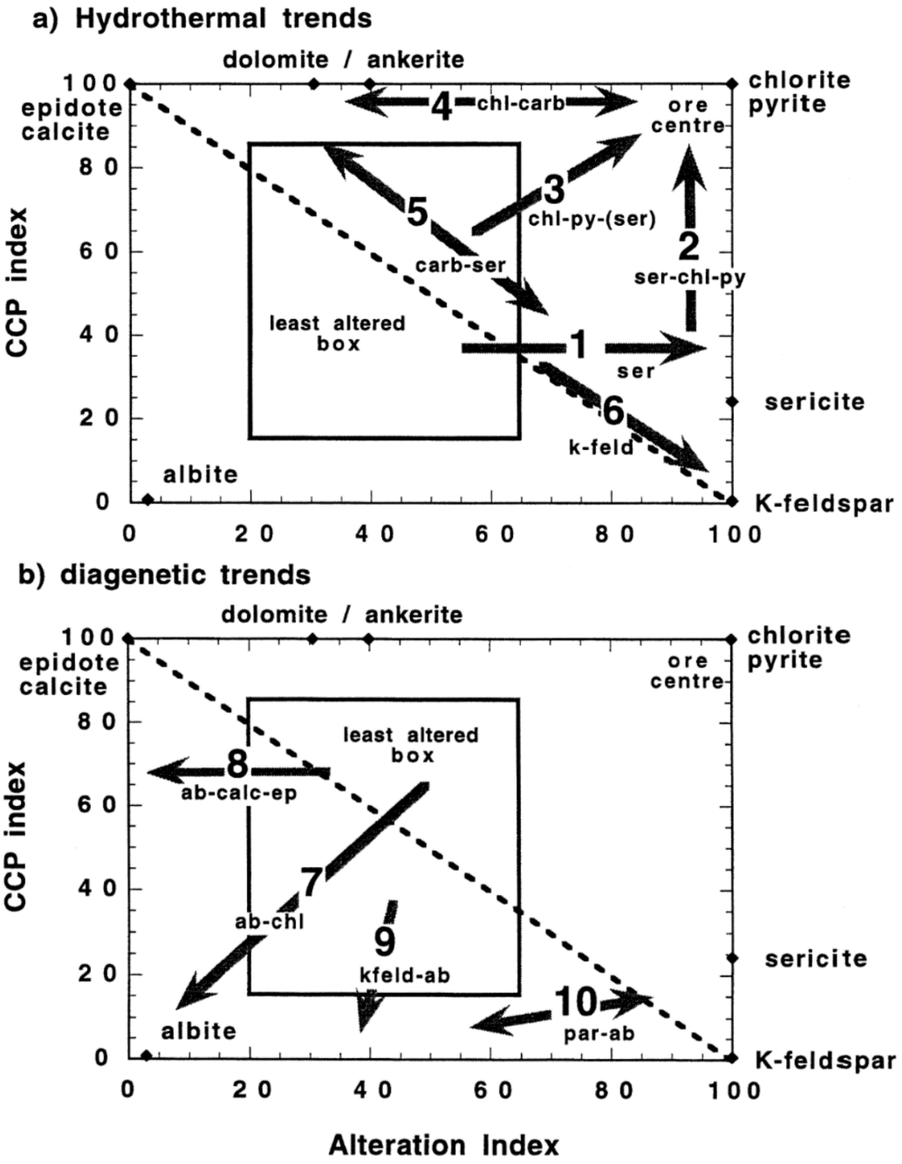

Figure 5.9. Hydrothermal (a) and diagenetic (b) trends of alteration connected with volcanic-hosted massive sulfide deposits represented in the alteration boxplot by Large et al. (2001). Fields for diagenetic alteration (lower left) and hydrothermal alteration (upper right)

Dominant alteration mineral is quartz followed by sericite, chlorite and epidote – Al-bearing phases. The abundance of Al-bearing alteration minerals is limited by the initial amount of Al in the rock (MacLean and Hoy, 1991; Barrett and MacLean, 1991). Formation of carbonate depends on the presence of CO_2 in the fluid and on available amount of Ca. Albite represents Na in partially altered rocks, except for minor Na in sericite but essentially all Na is mobilized and flushed from the system at higher water/rock ratios (Barrett and MacLean, 1994).

Mineral assemblages produced by hydrothermal alteration can vary in geological record due to late processes, which affected already formed massive sulfide body. They include mainly various grades of metamorphism (Table 5.4).

Table 5.4. Main minerals of hydrothermal alteration connected with VHMS deposits at different metamorphic grades. (Bonnet and Corriveau, 2007).

Alteration type	**Diagnostic minerals: unmetamorphosed deposits**	**Diagnostic minerals: greenschist facies**	**Diagnostic minerals: granulite facies**
Advanced argillic	Kaolinite, alunite, opal, smectite	Kaolinite, pyrophyllite, andalusite, corundum, topaz	Sillimanite, kyanite, quart
Argillic	Sericite, illite, smectite, pyrophyllite, opal	Sericite, illite, pyrophyllite	Sillimanite, kyanite, quartz, biotite, cordierite, garnet
Sericitic	Sericite, illite, opal	Sericite, illite, quartz	Biotite, K-feldspar, sillimanite, kyanite, quartz, cordierite, garnet
Chloritic	Chlorite, opal, quartz, sericite	Chlorite, quartz, sericite	Cordierite, orthopyroxene, orthoamphibole, phlogopite, sillimanite, kyanite
Carbonate propylitic	Carbonate (Fe, Mg), epidote, chlorite, sericite, feldspar	Carbonate (Fe, Mg), epidote, chlorite, sericite, feldspar	Carbonate, garnet, epidote, hornblende, diopside, orthopyroxene

Sulfide minerals at the VHMS bodies nascent from the hydrothermal fluids. Source of the metals were mainly surrounding host-rock, which was intensively leached by percolating hydrothermal fluids. Ability of sea-water to leach metals from rocks during hydrothermal activity has been postulated many times, and demonstrated experimentally (e.g. Bischoff and Dickson 1975; Seyfried and Bischoff 1981).Where the degree of exposure enables estimates of the volume of rock available for leaching metals, calculations show that there is plenty of protolith to supply the metals, even for the very large deposits (e.g. Stolz and Large 1992).

Stratification of sulfide minerals inside the massive sulfide body can be produced by the zone refining process (described by Ridley, 2012). The zone refining results from the periodic movement of high temperature fluids which preferentially incorporates phases precipitated earlier from lower temperature fluids. For instance, the preferential dissolution of Zn-S phases results in the zone purification of Cu-Fe-S ore. The overall effect is the preferential movement of major and trace elements along a thermal gradient that results in purification. Another results is that the concentration of trace elements are changed into economic grades at the low temperature part of the zone refining pathway. Zone refining provides a useful model for the explanation of sulfide mineral zoning inside the massive sulfide body (Galley et al., 2007).

5.2.2. Isotope geochemistry

Stable isotopes are often used in ore deposit studies to distinguish the sources of ore fluids (H, C, O, S), temperatures of ore deposition (S), and silicate alteration (O). When being used in studies focused on the volcanic-hosted massive sulfide deposits they are tools for distinguishing pathways of fluid movement (O), fluid origin (H, O, S), redox variations (C, S), and fluid phase separation (O, H) (Ridley, 2012).

Oxygen isotopes ($\delta^{18}O$) are being used (at the VHMS deposits) to indicate variations which are function of the alteration intensity. The lowest $\delta^{18}O$ are found at zones where the silicate alteration is the most intense. This usually corresponds to the central zone of sericitic alteration as reported from Japan (Green et al., 1983), Hercules, Tasmania (Green and Taheri, 1992), and Feitais-Estacao, Portugal (Barriga and Kerrich, 1984). The final value of alteration ($\delta^{18}O$) can be determined by number of variables - water/rock ratio, temperature of reaction, alteration mineralogy, initial bulk rock $\delta^{18}O$ value, fluid $\delta^{18}O$ (Taylor, 1977; Green et al., 1983). The stable isotopes of oxygen and hydrogen can be used for distinguishing different fluid sources (seawater and late stage magmatic fluid). This is possible due to their different $\delta^{18}O$ and δD values (approx. 0 per mil for seawater $\delta^{18}O$ and δD, 5 to 10 per mil $\delta^{18}O$ and -35 to -50 per mil δD for magmatic fluids) (Ridley, 2012). This statement is based on fact, that evaporation and fluid/rock interactions cannot produce that significant istopic variations, but mixing of magmatic fluid and seawater and (or) isoenthalpic boiling are both possible mechanisms (Ridley, 2012). The $\delta^{18}O$ values (that are used in calculations) have been measured in active seafloor hydrothermal systems (mean 0.91±0.37 per mil, 122 measurements; Shanks, 2001), in fluid inclusions in gangue quartz in ancient VHMS deposits (-0.7±1.75 per mil) (Ridley, 2012).

Because sulfur is the major element in the VHMS systems there are hundreds of analyses of the sulfur isotope ($\delta^{34}S$) composition. There is a significantly wider range of $\delta^{34}S$ values in the Phanerozoic sulfides compared to the Archean and Proterozoic sulfides (Ridley, 2012). This is closely paralleled the ancient seawater curve but was offset to lighter $\delta^{34}S$ values by about 18 per mil (described by Sangster, (1968) for the first time). That could implied different environmental conditions of formation (if the measured data are representative enough). Different $\delta^{34}S$ values (if samples are from one deposit) reflect mixing of light anoxic pore fluid with oxic seawater sulfate to produce sulfides with $\delta^{34}S$ values between -40 and -10 ppm (Ridley, 2012).

Nontraditional stable isotopes ($\delta^{11}B$, $\delta^{64}Cu$, $\delta^{66}Zn$, $\delta^{57}Fe$, $\delta^{82}S$) are being used for better understand the causes of isotopic fractionations and to distinguish the sources of metals.

5.2.3. Genetic model

Volcanic-hosted massive sulfide deposits form in sub-seafloor environment. Formation of a massive sulfide body starts with genesis and maturation of a sub-seafloor hydrothermal system (Fig. 5.10.). This system (described by Galley et al., 2007) is triggered by deep emplacement of a subvolcanic intrusion which leads to creation of an elongated rift zone or circular caldera. This leads to establishment of a low-temperature and shallow seawater convection system. This produce an extent shallow hydrothermal alteration and leads to formation of a hydrothermal exhalative sediments **(A)**. As the magma is protruding to the surface it produces deep-seated subseafloor seawater convection system. This system starts to leach metals from the host rock **(B)**. A largescale hydrothermal system is developed in which subhorizontal isotherms control the formation of semiconformable regional hydrothermal alteration assemblages. The high-temperature reaction zone next to the cooling intrusion is periodically breached due to seismic activity or dyke emplacement, allowing focused up flow of metal-rich fluids to the seafloor and their deposition **(C)**.

Formation of semi-massive to massive sulfide body (based on observations of modern sea-floor vents and hydrothermal systems, Miller et al., 1966) begins with growth of chimneys (smokers). These chimneys consist of silicate, sulfide and sulfate minerals, and are surrounded by breccias resulting from their mechanical collapse. The source of the sulfur in the VHMS deposits are sulfates from the seawater, which are reduced to form sulfides (Shanks, 2001). As the flow of hydrothermal fluids through the collapsed mound continues, a silica-, clay-, or sulfate-rich cap forms and seals the mound; at the Iberian Pyrite Belt this is represented by the jasper horizon of the Paraíso Formation (Relvas et al., 2011). In the sealed mound, the continuing deposition of sulfide minerals results in a massive sulfide body. The sequence of precipitation of the sulfide minerals from the fluid (about 300 ºC) is: *(i)* chalcopyrite; *(ii)* sphalerite + galena; *(iii)* manganese oxides an barite (Robb, 2005, pg. 197)

As the mound is growing, sulfide minerals are remobilized and form typical zonation of the massive sulfide bodies with copper enrichment at its base. Higher-temperature precipitating minerals replace those that precipitated at lower temperature. This process is referred as the zone refining (Eldridge et al., 1983).

This style of formation, with the black smokers, can be observed on a modern seafloor. Layered, stratiform deposits don’t have exact modern analogues (Robb, 2005, pg. 197). They can be result of a precipitation of a sulfide minerals in a distal place to its feeder zone (brine pools). Minerals are transported within “smoke” resulted from the black smoker.

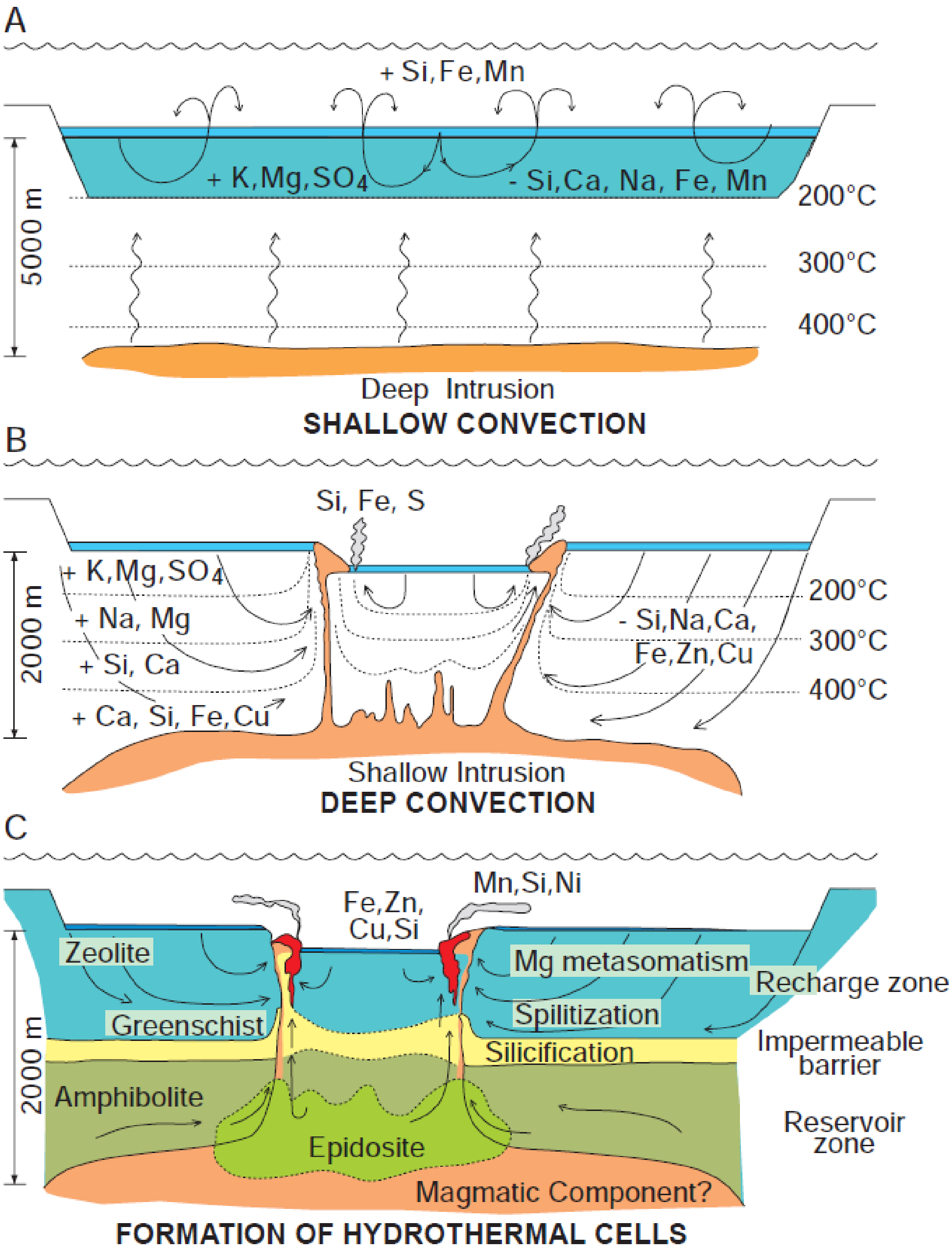

Figure 5.10. Formation and maturation and hydrothermal system which leads to formation of a massive sulfide body (Galley, 1993; Galley, 2007).

6. Conclusions

Both studied volcanic-hosted massive sulfide deposits that are situated in the Iberian Pyrite Belt show many similarities. Both were formed in the same age (ca 350 Ma), both are hosted by felsic volcanic rocks (within the Volcano-Sedimentary Complex) and are covered by jasper horizon and late Baixo-Alentejo Flysch Group. Because of their great tonnage (200 Mt of the Aljustrel and 350 Mt of the Neves-Corvo) they are interpreted to be results of a long-lived hydrothermal system and a particularly efficient deposition. At the Aljustrel deposit, jasper horizon may have acted as an impermeable cap (e. g. Barriga and Fyfe, 1988) which helped to the efficient deposition of the sulfide minerals and inhibited dispersion of them. This horizon is also present at the Neves-Corvo deposit thus it also may contribute to effective massive sulfide deposition. This is an evidence of a fact, that closed circulation of hydrothermal fluids is more effective in precipitating metals than the open ones.

Hydrothermal alteration shows same patterns at the both deposits. It includes chloritic alteration in the middle and envelopes of less intense sericitic alteration. At the Aljustrel deposit, the Albite zone is also present. This zone is missing at the Neves-Corvo due to enormous extent of the alteration zone.

Metals from the both deposits came mainly from the Phyllite-Quartzite group. Ore zonation (copper on the base, pyrite on the top of the sulfide body) from both deposits is a result of the zone refining process. It resulted in various zones with different main mineral – pyrite, chalcopyrite or sphalerite. This zones were established based on temperature of dissolution of the each sulfide mineral. At the Neves-Corvo deposit, there is much more chalcopyrite then at the Aljustrel deposit. This could be result of contribution of metals from a different source, than the Phyllite-Quartzite group. It is interpreted to be fluids and metals from a hidden magmatic intrusion of probably granitic composition – tin ores at the Neves-Corvo.

7. Acknowledgments

I would like to thank to my supervisor, David Dolejs for his help, guidance and patience with which he was answering all my questions. Then to Jorge Relvas for the opportunity that I was able to come to Portugal from the Czech Republic and to study the volcanic-hosted massive sulfide deposits of the Iberian Pyrite Belt on the Universidade de Lisboa with him. Also I would like to thank to João Carvalho for his help with the thin-sections and distinguishing opaque minerals under the microscope and to Luis Santos for his help with the microprobe analysis.

Big thanks goes to my family for supporting me in studying geology and to my girlfriend for not killing me while I was explaining to her what I am doing.

8. References

Adamides N.G. (2010): Mafic-dominated volcanogenic sulphide deposits in the Troodos ophiolite, Cyprus Part 2 – a review of genetic models and guides for exploration. Applied Earth Science (Transactions of the Institution of Mining and Metallurgy) B 119, 193-204.

Allen R.L., Weihed P. (2002): Global comparisons of volcanic-associated massive sulphide districts. Geological Society London Special Publication 204, 13-37.

Almodóvar G.R., Sáez R., Pons J.M., Maestre A., Toscano M., Pascual E. (1998): Geology and genesis of the Aznalcollar massive sulphide deposits Iberian Pyrite Belt, Spain. Mineralium Deposita 33: 111– 136.

Barrett T.J., and MacLean W.H. (1991): Chemical, mass and oxygen isotope changes during extreme chloritization and sericitization of an Archean rhyolite, Noranda area. Economic Geology, v. 86, p. 406-414.

Barrett T.J., MacLean W.H., (1994): Chemostratigraphy and hydrothermal alteration in exploration for VHMS deposits in greenstones and younger rocks, in Alteration and Alteration Processes Associated with Ore-Forming Systems, (ed.) D.R. Lentz; Geological Association of Canada, Short Course Notes Volume 11, p. 433-467.

Barrett T.J., MacLean W. H. (1998): Chemostratigraphy and Hydrothermal Alteration in Exploration for VHMS Deposits in Greenstones and Younger Volcanic Rocks. Short Course Notes, v. 11, 433-467.

Barrie C.T., and Hannington M.D. (1999): Introduction: Classification of VMS deposits based on host rock composition, *in* Barrie, C.T., and Hannington, M.D., eds., Volcanic-Associated Massive Sulfide Deposits: Processes and Examples in Modern and Ancient Settings. Reviews in Economic Geology, v. 8, p. 2-10.

Barrie C.T., Amelin Y., Pascual E. (2002): U-Pb Geochronology of VMS mineralization in the Iberian Pyrite Belt. Mineralium Deposita 37:684-703.

Barriga F.J.A.S. (1983): Hydrothermal metamorphism and ore genesis at Aljustrel, Portugal. Umpub PhD Thesis, University of Western Ontario, Ontario, Canada 386 pp.

Barriga F.J.A.S., Kerrich R. (1984): Extreme ^{18}O-enriched volcanics and ^{18}O-evolved marine water, Aljustrel, Iberian Pyrite Belt: transition from high to low Rayleigh number convective regimes. Geochim Cosmochim Acta 48: 1021-1031.

Barriga F.J.A.S., Fyfe W.S. (1988): Giant pyritic base-metal deposits: the example of Feitais (Aljustrel, Portugal). Chemical Geology 69: 331±343.

Bischoff J. L., Dickson F. W., (1975): Earth Planetary Science Letters 25: 385.

Bonnemaison M., Braux C., Joubert M., Mercier F. (1993): Estudio con técnica de gestión n de multicriterios en la investigación de sulfuros polimetálicos: Herrerias, antiforma de Puebla de Guzmán (Huelva, España). Symp. Polymetallic Sulphides of the Iberian Pyrite Belt, Evora, Portugal, pp 1.5.1±1.5.14.

Bonnet A.L. and Corriveau L. (2007): Alteration vectors to metamorphosed hydrothermal systems in gneissic terranes, in Goodfellow, W.D., ed., Mineral deposits of Canada—A synthesis of major deposit-types, district metallogeny, the evolution of geological provinces, and exploration methods. Geological Association of Canada, Mineral Deposits Division, Special Publication No. 5, p. 1035–1049.

Carvalho D., Barriga F.J.A.S., Munhá J. (1999): Bimodal-siliciclastic systems - the case of the Iberian Pyrite Belt. Reviews in Economic Geology 8:375-408.

Cathelineau M. (1988): Cation site occupancy in chlorites and illites as a function of temperature. Clay Minerals 23: 471-485.

Constantinou B. and Govett G.J.S. (1978): Geology, geochemistry, and genesis of Cyprus sulfide deposit. Economic Geology 68, 843-858.

DeMatties T.A. (1994): Early Proterozoic volcanogenic massive sulfide deposits in Wisconsin: and overview. Economic Geology 89, 1122-1151.

Eckstrand O.R., Sinclair W.D. and Thorpe R.I., eds. (1995): Geology of Canadian Mineral Deposit Types, Geology of Canada, No. 8, Decade of North American Geology (DNAG). Geological Society of America, Part 1, p. 183-196.

Eldridge C.S., Barton P.B., Ohmoto, H. (1983): Mineral textures and their bearing on formation of the Kuroko orebodies: Economic Geology Monography 5: 241-281.

Fernandes Ana S.C., Relvas Jorge M.R.S., Matos João X. (2013): Hydrothermal alteration zonation in the massive sulfide-hosting footwall sequence of Lousal, Iberian Pyrite Belt. Congresso Nacional de Jovens Investigadores em Geociências, LEG 2011.

Franklin J.M., Gibson H.I., Jonasson I.R., Galley A.G. (2005): Volcanogenic massive sulphide deposits. Economic Geology, 100th Anniversary Volume, 523-560.

Franklin J.M., Lydon J.W. and Sangster D.F. (1981): Volcanic-associated massive sulfide deposits; in Skinner, B.J. (eds.). Economic Geology 75th Anniversary Volume: Society of Economic Geologists, p. 485-627.

Franklin J.M., Gibson H.L., Jonasson I.R. and Galley A.G. (2005): Volcanogenic Massive Sulfide Deposits, *in* Hedenquist, J.W., Thompson, J.F.H., Goldfarb, R.J., and Richards, J.P., eds., Economic Geology 100th Anniversary Volume: The Economic Geology Publishing Company, p. 523-560.

Galley A.G., Bailes A.H., Kitzler G. (1993): Geological setting and hydrothermal evolution of the Chisel Lake and North Chisel Zn-Pb-Ag-Au massive sulphide deposit, Snow Lake, Manitoba. Exploration and Mining Geology, v. 2: 271-295.

Galley A., Hannington M., Jonasson I. (2007): Volcanogenic massive sulphide deposits. – In: Goodfellow W. D. (eds.). Mineral deposits of Canada, 141-161.

García Palomero F. (1980): Caracteres geológicos y relaciones morfológicas y genéticas de las mineralizaciones del Anticlinal de Riotinto. Inst Estud Onubenses ``Padre Marchena'', Excma Diputación Provincial de Huelva, 264 pp.

García Palomero F. (1992): Mineralizaciones de Riotinto (Huelva): Geología, génesis y modelos geológicos para su explotación y evaluación de reservas mineras. In: García Guinea J., Martínez Frías J. (eds) - Recursos Minerales de Espana. CSIC, Madrid, 1325-1351.

Gemmell J.B., and Large R.R. (1992): Stringer system and alteration zones underlying the Hellyet volcanic-hosted massive sulfide deposit, Tasmania, Australia: Economic Geology 87, p. 620-649.

Gemmell J.B., Large R.R., Zaw K. (1998): Palaeozoic volcanic-hosted massive sulphide deposits. Journal of Australian Geology & Geophysics 17, 129-137.

Gibson H.L., and Watkinson D.H. (1990): Volcanogenic massive sulphide deposits of the Noranda cauldron and shield volcano, Quebec: The Northwestern Quebec Polymetallic Belt: A Summary of 60 Years of Mining Exploration,.Canadian Institute of Mining and Metallurgy Special Volume 43, p. 119–132.

Gifkins C., Herrmann W., Large R. (2005): Altered volcanic rocks: a guide to description and interpretation. Hobart, Tasmania, Australia: Centre for Ore Deposit Research, 275 pgs.

Green G.R., Solomon M. and Walshe J.L, (1981): The formation of the volcanic-hosted massive sulfide ore deposit at Rosebery, Tasmania. Economic Geology, v.76, p. 304–338.

Gumiel P., Sanderson DJ., Campos R., Roberts S. (2001): Fractal geometry of the Cerro Colorado stockwork, Rio Tinto Mine, Iberian Pyrite Belt. In: Tornos, F., Pascual, E., Sa´ez, R., Hidalgo, R. (Eds.), GEODE Workshop Massive Sulphide deposits in the Iberian Pyrite Belt: New Advances and Comparison with Equivalent Systems, pp. 23–24.

Hannington M.D., Bleeker W., Kjarsgaard I. (1999): Sulfide mineralogy, geochemistry, and ore genesis of the Kidd Creek deposit: Part II. The bornite zone: Economic Geology Monograph, 10, p. 225-266.

Herzig P.M., Hannington M.D. (1995): Polymetallic massive sulfides at the modern seafloor – A review. Ore Geology Reviews 10, 95-115.

Ishikawa Y., Sawaguchi T., Ywaya S., Horiuchi M. (1976): Delineation of prospecting targets for Kuroko deposits based on modes of volcanism of underlying dacite and alteration haloes. Mining Geology, Volume 26, pages 105-117.

Jorge R.C.G.S., Pinto A.M.M., Tassinari C.C.G., Relvas J.M.R.S., Munhá J. (2007): VHMS metal sources in the Iberian Pyrite Belt: new insights from Pb isotope data, in Andrew et al. (eds.). Digging Deeper, Special Publication of the Irish Association for Economic Geology: 1097-1100.

Khin Zaw, Sutherland F.L., Dellapasqua F., Ryan C.G., Yui T-F., Menargh T.P., Duncan D. (2006): Contrasts in gem corundum characteristics, eastern Australian basalt fields: trace elements, fluid/melt inclusions and oxygen isotopes. Mineralogical Magazine 70: 669-687.

Laird J. (1988): Chlorites: metamorphic petrology. in: Hydrous Phyllosilicates (Exclusive of Micas) (S.W. Bailey, editor). Reviews in Mineralogy, Mineralogical Society of America, Washington, DC, 19 405-447.

Lanari P., Wagner T., Vidal O. (2014): A thermodynamic model for di-trioctahedral chlorite from experimental and natural data in the system MgO–FeO–Al2O3–SiO2–H2O: applications to P–T sections and geothermometry. Contribution to Mineral Petrology 167:968.

Large R.R. (1992): Australian volcanic-hosted massive sulphide deposits: features, styles and genetic models. Economic Geology, v. 87, p. 471-510.

Large D.E. & Walcher E. (1999): The Rammelsberg Massive Sulphide Cu-Zn-Pb-Ba deposit, Germany: an example of sediment-hosted, massive sulphide mineralisation. Mineralium Deposita, 34: 522-538.

Large R.R., Gemmell J.B., Paulick H. (2001): The alternation box plot: A simple approach to understanding the relationship between alteration mineralogy and lithogeochemistry associated with volcanic-hosted massive sulfide deposits. Economic Geology 96 (5): 957-971.

Leistel J.M., Bonijoly D., Braux C., Freyssinet Ph., Kosakevitch A., Leca X., Lescuyer J.L., Marcoux E., Milési J.P., Piantone, P., Sobol F., Tegyey M., Thiéblemont D., Viallefond

L. (1994): The massive sulphide deposits of the South Iberian Pyrite Province, geological setting and exploration criteria. Editions BRGM 234.

Leistel J.M., Marcoux E., Thiéblemont D., Quesada C., Sánchez A., Almodóvar G.R., Pascual E. and Sáez R. (1998): The volcanic-hosted massive sulphide deposits of the Iberian Pyrite Belt. Mineralium Deposita, v. 33, p. 2-30.

Lydon J.W. (1988): Ore deposit models #14, volcanogenic massive sulphide deposits Part 2: Genetic models. Geoscience Canada 15: 43-65.

MacLean W.H. and Hoy L.D. (1991): Geochemistry of hydrothermally altered rocks at the Horne Mine, Noranda, Quebec. Economic Geology, v. 86, p. 506-528.

Maia F., Pinto C., Waerenborgh J.C., Gonçalves M.A., Prazeres C., Carreira O., Sério S. (2012): Metal partitioning in sediments and mineralogical controls on the acid mine drainage in Ribeira da Água Forte (Aljustrel, Iberian Pyrite Belt, Southern Portugal). Applied Geochememistry 27, 1063–1080.

Marcoux E. (1998): Lead isotope systematics of the giant massive sulphide deposits in the Iberian Pyrite Belt. Mineralium Deposita 33: 45-58.

McKee G.S., Hidalgo R., Ixer R.A., Boyce A., Guerrero V. Pons J.M. (2001): Deposit formation and structural evolution at Aguas Tenidas Este. In: Tornos, F., Pascual, E., Sáez, R., Hidalgo, R. (Eds.), GEODE Workshop Massive Sulphide Deposits in the Iberian Pyrite Belt: New Advances and Comparison with Equivalent Systems, pp. 38-89.

Miller A. R., Densmore C. D., Degens E. T., Hathaway J. C., Manheim F. T., McFarlin P. F., Pocklington R., and Jokela A. (1966): Hot brines and recent iron deposits in deeps of the Red Sea. Geochimica and Cosmochimica Acta 30, 341–359.

Moreno C. (1993): Postvolcanic Paleozoic of the Iberian Pyrite Belt: an example of basin mophologic control on sediment distribution in a turbidite basin. Journal of Sedimentary Petrology 63: 1118±1128.

Mosier Dan L., Singer Donald A., Berger Vladimir I. (2007): Volcanogenic Massive Sulfide Deposit Density. USGS Survey Scientific Investigations Report 2007-5082

Munhá J. and Kerrich, R. (1981): Sea water-basalt interaction in spilites from the Iberian pyrite belt. Contributions to Mineralogy and Petrology, v. 75, p. 15–19.

Munhá J., Barriga F.J.A.S., and Kerrich, R., (1986): High $_{18}$O ore-forming fluids in volcanic-hosted base metal massive sulfide deposits: Geologic, $_{18}$O/$_{16}$O, and D/H evidence from the Iberian pyrite belt, Crandon, Wisconsin, and Blue Hill, Maine. Economic Geology, v. 81, p. 530–552.

Munhá J., Relvas J.M.R.S., Barriga F.J.A.S., Conceição P., Jorge,R.C.G.S., Mathur R., Ruiz J., Tassinari C.C.G. (2005): Os Isotopes Systematics in the Iberian Pyrite Belt. In: Mao, J. and Bierlein, F. (Eds.), 8th SGA Meeting, Beijing, China. Springer, p 663-666.

Ohmoto H. (1996): Formation of volcanogenic massive sulfide deposits: The Kuroko perspective. Ore Geology Reviews 10, 135-177.

Oliveira J.T. (1983): The marine Carboniferous of South Portugal: a stratigraphic and sedimentological approach. In: Lemos de Sousa M.J., Oliveira J.T. (eds) The Carboniferous of Portugal. Mémoires du Service géologique. Port 29: 3±37.

Oliveira V., Matos J., Bengala J., Silva M., Sousa P., Torres L. (1993): Lagoa Salgada um novo depósito na F.P.I., Bacia Terciaária do Sado. Est Not Trap. Institute of Geology and Mineralogy 35: 55±89.

Oliveira V., Matos J., Bengala J., Silva M., Sousa P., Torres L. (1998): Geology and Geophysics as successful tools in the discovery of the Lagoa a Salgada orebody (Sado Tertiary Basin-Iberian Pyrite Belt), Grándola, Portugal. Mineralium Deposita 33: 170±187.

Oliveira J.T., Relvas J.M.R.S., Pereira Z., Matos J.X., Rosa C., Rosa D., Munhá J., Jorge R., Pinto A. (2006): O Complexo vulcanosedimentar da Faixa Piritosa: estratigrafia, vulcanismo, mineralizações associadas e evolução tectono-estratigráfica no contexto da zona Sul-Portuguesa. In: Dias R, Araújo A, Terrinha P, Kulberg JC (eds) Geologia de Portugal no contexto da Ibéria, Universidade de Évora, Portugal, pp 207-244.

Quesada C. (1998):. A reappraisal of the structure of the Spanish segment of the Iberian Pyrite Belt. Mineralium Deposita 33: 31– 44.

Piercey S.J. (2010): An overview of petrochemistry in the regional exploration for volcanogenic massive sulphide deposits. – Geochemistry: Exploration, Environment, Analysis 10, 1-18.

Piercey S.J. (2011): The setting, style, and role of magmatism in the formation of volcanogenic massive sulfide deposits. Mineralium Deposita 46, 449-471.

Pinedo Vara I. (1963): Piritas de Huelva. Su historia, minería a aprovechamiento. Summa, Madrid, 1003 pp.

Pinto A., Relvas J.M.R.S., Barriga F.J.A.S., Scott S.D. (2005): Gold mineralization in recent and ancient volcanic-hosted massive sulphides: the PACMANUS field and the Neves-Corvo deposit. In: Mao, J. and Bierlein, F. (Eds.), 8th SGA Meeting, Beijing, China. Springer, p 683-686.

Pisutha-Arnond V. and Ohmoto H. (1983): Thermal history, and chemical and isotopic compositions of the ore-forming fluids responsible for the Kuroko massive sulfide deposits in the Hokuroku district of Japan. Economic Geology, Monograph 5: 523-558.

Ramírez J., Rosales F., Maroto S., Bellamy J. (1988): Metodología de la investigación n que ha dado lugar al descubrimiento de una nueva masa de sulfuros al SO de Valverde del Camino (Faja Pirítica de Huelva). Estado actual de conocimientos. Proc VIII Congreso Internacional Minería y Metalurgía. Oviedo 7: 251±273.

Relvas J.M.R.S., Barriga F. J. A. S., Ferreira A., Noiva P. C., Pacheco N., Barriga G. (2006): Hydrothermal alteration and mineralization in the Neves-Corvo volcanic-hosted massive sulfide deposit, Portugal. I. Geology, mineralogy, and geochemistry. Economic Geology 101, 753-790.

Relvas J.M.R.S., Jorge R.C.G.S., Pinto A.M.M., Carvalho J., Marques A.F.A., Gaspar M., Barriga F.J.A.S., Rosa C., (2009): Recent Advances in Understanding Mineralizing Processes in the Iberian Pyrite Belt, in P. J. Williams et al. (eds), Smart Science for Exploration and Mining, Published by Economic Geology Research Unit, James Cook University, Townsville, Australia: 481-483.

Relvas J.M.R.S., Barriga F.J.A.S., Carvalho .J.R.S., Pinto A.M.M., Matos J.X., Rosa C.J.P., Pereira Z. (2011): Structure, stratigraphy and hydrothermal alteration at the Gavião orebodies, Aljustrel: reconstruction of a dismembered ore-forming system at the Iberian Pyrite Belt and implications for exploration. Let's Talk Ore Deposits, 11th Biennial SGA Meeting, 26-29th September, 2011, Antofagasta, Chile: pp. 772-774.

Ridley, John. Ore deposit geology. 1st pub. Cambridge: Cambridge University Press, 2013, 398.

Ridley W. Ian (2012): Geochemical characteristics in volcanogenic massive sulfide occurrence model: U.S. Geological Survey Scientific Investigations Report 2010–5070 –C, chap. 14, 18 p.

Rieder M., Cavazzini G., D’yakonov YuS., Frank-Kamenetskii V.A., Gottardi G., Guggenheim S., Koval’ P.V., Müller G., Neiva A.M.R., Radoslowich E.W., Robert J.L., Sassi F.P., Takeda H., Weiss Z., Wones D.R. (1998): Nomenclature of the micas. Canadian Mineralogist 36: 905-912.

Riverin G., Hodgson C. J. (1980): Wall-rock Alteration at the Millenbach Cu-Zn Mine, Noranda, Quebec, Economic Geology, v 75, p. 424-444.

Robb, L. Introduction to ore-forming processes. 1st pub. Malden, Mass: Blackwell Publishing, 2005, viii, 373.

Rona P.A. (1988): Hydrothermal mineralization at oceanic ridges. Canadian Mineralogist 26: 431±466.

Routhier P., Aye F., Boyer C., Lécolle M., Moliere E.P., Picot P., Roger G. (1978): La Ceinture Sud-Ibérique á amas sulfuré s dans sa partie espagnole mediane. Mém BRGM 94: 265 pp.

Ruiz de Almodóvar G., Pascual E., Marcoux E., Sáez R., Toscano M. (1994): Mineralogía de las zonas de alteración cloríticas asociadas a los sulfuros masivos del área de Aznalcóllar. Boletin de la Sociedad Espanola de Mineralogía17. 163-165.

RTZ (1996): RTZ exploration in the Pyrite Belt. Simposio Sulfuros Polimetálicos de la Faja Pirítica Ibérica, Huelva, 21±23 eb 1996, 4 pp.

Sáez R., Pascual E., Toscano M., Almodóvar G. R. (1999): The Iberian type of volcano-sedimentary massive sulphide deposits. Mineralium Deposita 34, 549-570.

Sanchez-España J, Velasco F, Yusta I. (2000): Hydrothermal alteration of felsic volcanic rocks associated with massive sulphide deposition in the Northern Iberian Pyrite Belt (SW Spain). Applied Geochemistry15: 1265-1290.

Sato T. (1997): Kuroko deposits: their geology, geochemistry and origin, In Volcanic Processes in Ore Genesis, Anon, (ed.), London, Institution of Mining and Metallurgy, pp. 153-161.

Schermerhorn L.J.G., Stanton W.I. (1969): Folded overthrusts at Aljustrel (South Portugal) Geologiccal Magazine 106: 130±141.

Schutz W., Dulski P., Germann K. (1988): Geochemical features of magmatic evolution and ore deposition in the Pyrite Belt of Southern Spain. In: Freidrich, G.H., Herzig, P.M. (Eds.), Base Metal Sulfide Deposits. Springer-Verlag, Berlin – 240-253.

Seyfried, W.E., Bischoff, I.L. (1981): Experimental seawater-basalt interaction at 300'C, 500 bars: Chemical exchange, secondary mineral formation and implications for the transport of heavy metals. Geochimica and Cosmochimica Acta 45, 135-149

Shanks W. C., III. (2001): Stable isotopes in seafloor hydrothermal systems; vent fluids, hydrothermal deposits, hydrothermal alteration, and microbial processes. Reviews in Mineralogy and Geochemistry 43: 469-525

Solomon M. & Groves D.I. (1994): The geology and origin of Australia’s mineral deposits. Oxford Monographs on Geology and Geophysics 28.

Solomon M., Quesada C., (2003): Zn-Pb-Cu massive sulfide deposits: Brine-pool types occur in collisional orogens, black smoker types occur in backarc and/or arc basins: Geology, v. 31, p. 1029–1032.

Stix J., Kennedy B., Hannington M., Gibson H., Fiske R., Mueller W., Franklin J. (2003): Caldera-forming processes and the origin of submarine volcanogenic massive sulfide deposits. Geology 31, 375-378.

Stolz, A.J., Large, R.R. (1992): Evaluation of the sonrce rock control on precious metal grades in volcanic-hosted massive sulphide deposits from western Tasmania. Economic Geology 87: 720-738.

Strauss G.K., Madel J. (1974): Geology of massive sulphide deposits in the Spanish-Portuguese Pyrite Belt. Geologische Rundschau 63: 191±211.

Syme E.C., and Bailes A.H. (1993): Stratigraphic and tectonic setting of Early Proterozoic volcanogenic massive sulfide deposits, Flin Flon, Manitoba. Economic Geology, v. 88, p. 566–589.

Tornos F., Gonzalez Clavijo E., Spiro B. (1998): The Filón Norte orebody, Tharsis, Iberian Pyrite Belt: a proximal low-temperature shale-hosted massive sulphide in a thin-skinned tectonic belt. Mineralium Deposita 33: 150–169.

Tornos F., Casquet C. and Relvas J.M.R.S. (2005): Transpressional tectonics, lower crust decoupling and intrusion of deep mafic sills: A model forthe unusual metallogenesis of SW Iberia. Ore Geology Reviews, v. 27, p. 133–163.

Tornos F., (2006): Environment of formation and styles of volcanogenic massive sulfides: The Iberian Pyrite Belt: Ore Geology Reviews, 28, p. 259-307.

Toscano M., Almodóvar G.R., Sáez R., Pascual E. (1993) Hydrothermal alteration related to the "Masa Valverde" massive sulphide deposit, Iberian Pyrite Belt, Spain. In: Fenoll Hach-Ali P, Torres-Ruiz J, Gervilla F. (Eds.), Current research in geology applied to ore deposits, University of Granada, Spain, 389-392.

Vearncombe S., Barley M.E., Groves D.I. (1995): 3.26 Ga black smoker-type mineralization in the Strelley Belt, Pilbara Craton, Western Australia. Journal of the Geological Society London 152:587–590.

Velasco F., Sánchez Espana J., Boyce A., Fallick A.E., Sáez R., Almodóvar G.R. (1998): A new sulphur isotopic study of some Iberian Pyrite Belt deposits: evidence of a textural control on some sulphur isotope compositions. Mineralium Deposita 34: 1-18.

Zhang X.C., Spiro B., Halls C., Stanley C., Yang, K.Y. (2003): Sediment-hosted disseminated gold deposits in southwest Guizhou, PRC: Their geological setting and origin in relation to mineralogical, fluid inclusion, and stable-isotope characteristics: International Geology Review, v. 45, p. 407–470.